7

Juxtacellular Labeling of Individual Neurons In Vivo: From Electrophysiology to Synaptology

ALVARO DUQUE and LASZLO ZABORSZKY

ALVARO DUQUE • Department of Neurobiology, Yale University School of Medicine, New Haven, CT 06510 LASZLO ZABORSZKY • Center for Molecular and Behavioral Neuroscience, Rutgers, The State University of New Jersey, Newark, NJ 07102

Abstract: This chapter summarizes details pertaining to the extracellular recording and juxtacellular labeling method and its application to the characterization of basal forebrain neurons. Juxtacellular labeling is compared to other single-cell labeling techniques. Compatibility of the method with fluorescent retrograde/anterograde neural tracing, immunohistochemical, and electron microscopy techniques is also illustrated.

Keywords: basal forebrain, 3D reconstruction, electron microscopy, morphology, neurochemical identification

I. INTRODUCTION

Brain regions consist of elementary local circuits and cell assemblies specialized to carry out discrete computations that eventually give rise to behavior. These circuits are built from regionally specific combinations of limited types of individual neurons (see Nadasdy *et al.*, this volume). However, depending on the computational needs of the brain regions and the particular electrophysiological, neurochemical, and hodological characteristics of different neuronal populations, these circuits become increasingly complex across the neuraxis. Except for a few heuristic attempts by Cajal (1911) in the early part of the twentieth century, it was only in the 1970s when the imaginative cerebellar and cortical circuitry models of Szentágothai were published (Szentágothai, 1970, 1978). These general models were based on correlating (mostly indirectly) the 3D spatial architecture, derived from Golgi studies, with the synaptic pattern of putative circuits obtained from electron microscopical analysis (see also Arbib *et al.*, 1998, and partial list of Szentágothai's publications in Zaborszky *et al.*, 1992). To correctly interpret the complex entanglement of axons and dendrites under the electron microscope, however, it was necessary to combine the full cell visualization of the Golgi method (Golgi, 1883) with the power of electron microscopy to resolve individual synapses. After the initial attempt of Blackstad (1965), the development of gold toning of Golgi impregnated neurons (Fairen *et al.*, 1977) paved the way to identify the synaptic connections of individual neurons (Somogyi, 1977).

A further development in the analysis of neural circuits was the combination of intracellular electrophysiological recordings with horseradish peroxidase (HRP) labeling of the recorded cell (Jankowska *et al.*, 1976; Kitai *et al.*, 1976a, b; Light and Durkovic, 1976; Snow *et al.*, 1976; Cullheim and Kellerth, 1978). HRP, introduced as a neuroanatomical tracer in the early 1970s (Kristensson and Olsson; 1971; LaVail and LaVail, 1972), is an enzyme that catalyzes the reaction by which diaminobenzidine (DAB) precipitates and forms an electron-dense product (Graham and Karnovsky, 1966). The chapters of Somogyi and Freund in the previous edition of this series are excellent reviews on the study of the synaptic relationships of interconnected and chemically identified neurons, using a combination of electrophysiology, HRP filling, Golgi method (Golgi, 1883), and immunocytochemistry (Freund and Somogyi, 1989; Somogyi and Freund, 1989).

Intracellular recordings can also be combined with fluorescent dye labeling and histochemical or immunocytochemical methods to identify the transmitter of the recorded neurons (Aghajanian and Vandermaelen, 1982; Grace and Bunney, 1983a, b). However, morphological reconstructions of these neurons and study of their synaptology require conversion of the fluorescent signal to a permanent DAB end product (Buhl, 1993), a fact that makes this avenue much too cumbersome to be routinely applied.

In vivo technical advances, including the use of voltage-sensitive or calcium-sensitive dyes, for the study of individual synapses in the living animal as described in the chapter of Goldberg *et al.* (this volume) have the disadvantage of being applicable only to superficial layers of the cortex. Hence, they are not useful for investigating deep subcortical structures such as the basal forebrain or the basal ganglia. Intracellular or patch recordings are difficult to apply in vivo when the neuron to be recorded and labeled is in a deep subcortical structure or in an area densely packed with neuropil and fibers. The chances of breaking the fine pipette tips used for intracellular recordings increase dramatically as a function of the distance traveled by the micropipette electrode. Moreover, in vivo intracellular approaches are limited by the stability of the preparation. In particular, respiration and heartbeat produce movement, which is not reduced or only minimally reduced by the use of vibration-free tables. Movement in the preparation compromises the integrity of the micropipette tip, disrupts the recording, and usually quickly kills the cell under investigation. Therefore, most intracellular or patch recordings involving single-cell labeling in the basal forebrain or basal ganglia have taken place in vitro (Alonso *et al.*, 1996; Nambu and Llinas, 1997; Koos and Tepper, 1999, 2002). In vitro preparations are very stable and have, therefore, revealed much about intrinsic electrophysiological properties of these neurons, but the nature of the preparation usually does not allow full morphological reconstructions or chemical identification. Cutting afferents and efferents, however, and maintaining the neuron alive under typical in vitro conditions raises questions as to the validity and relevance of some of the results obtained. Moreover, behavioral correlates such as electroencephalograph (EEG) cannot be obtained in vitro.

In vivo extracellular recordings are usually easier to perform than intracellular recordings. However, for many years a major obstacle in their usefulness was the inability to label the recorded cell. A first approach to resolve this problem was to eject a dye, such as HRP, at the end of the recording session and label a small group of cells found in close proximity to the pipette tip. This effort, however, fell short of identifying "the recorded cell" although it did identify a small area where the recording took place. By decreasing the tip size (to 1–4 μm) of glass microelectrodes filled with 0.5–1.0% HRP in 2 M NaCl and ejecting HRP with 400–1000 nA negative current for 5–25 s after regular extracellular recordings, 30 years ago Lynch and colleagues (Lynch *et. al.*, 1974a, b) managed to label only 1–4 cells per attempt. However, in cases in which only one neuron was labeled, no evidence was provided that the stained neuron was actually the one recorded from. Twenty years later, working in the thalamic reticular nucleus, Pinault (1994) described a method for recording and labeling single neurons extracellularly and for the first time provided evidence that the labeled cell was the one recorded from. The usefulness of this methodology, called juxtacellular labeling, was finally established by Pinault in a 1996 study, which presented further evidence from different rat brain areas, including the neocortex, thalamus, basal ganglia, basal forebrain, and cerebellum, that the juxtacellularly labeled neuron was the one previously recorded from.

In this chapter we describe juxtacellular labeling of single neurons with details based on our own experience, using the method mostly in the basal forebrain of the rat. We will present our own control experiments providing further supporting evidence for the validity of the technique. We will elaborate on the usefulness of the technique by illustrating the compatibility of the labeling procedure with various tracer and immunocytochemical methods both at the light and at the electron microscopical levels to study the synaptology of chemically and electrophysiologically identified neurons, whose activity is also correlated with EEG recordings. The advantages, limitations, and drawbacks of the technique are also discussed.

II. GENERAL METHODOLOGY

Lesions or injections of anterograde and retrograde tracers may be applied prior to recording and labeling of single neurons (see section "Tracer Techniques in Combination with Electrophysiological Recording and Juxtacellular Labeling"). These extra steps can substantially increase the amount of information collected from a single neuron. These and all other procedures involving animals, and details pertaining to animal treatment should be in strict accordance with National Institutes of Health guidelines, which are readily available in publications such as the "Guide for the Care and Use of Laboratory Animals." Before starting any experiments, protocols need to be reviewed and approved by the respective Institutional Animal Care and Use Committee (IACUC). Figure 7.1 illustrates the general methodology.

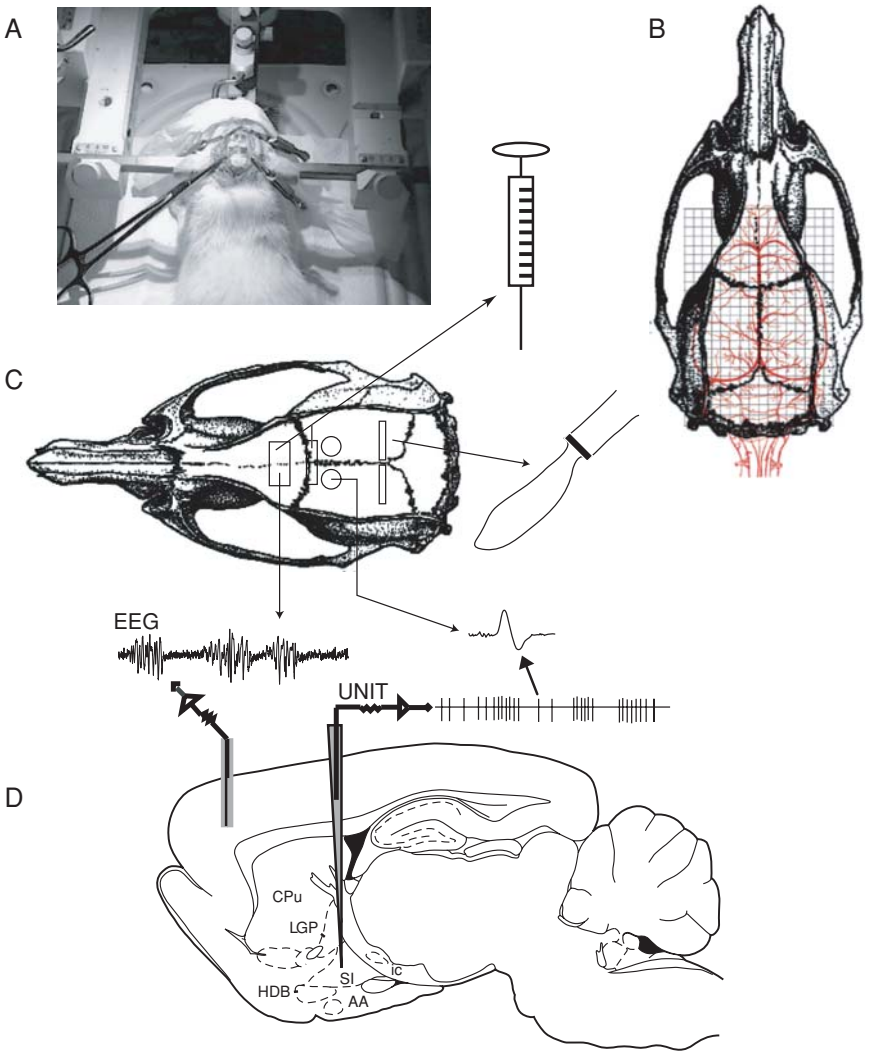

Figure 7.1. Schematic diagram of general methodology. (A) shows a digital photograph of the head of a rat fixed in a stereotaxic apparatus; four open holes on the cranium are visible. (B) shows a diagram of the rat skull with the superficial venous system superimposed on it. Special care is always taken to avoid rupture of the veins to minimize bleeding, and mediolateral measurements are taken from the midline of the superior sagittal sinus instead of from the midline of the bone fissure. (C) illustrate different procedures, some of which like the injection of tracers or other chemicals and the infliction of cuts or other lesions can be performed hours or days before recording and juxtacellular labeling of single neurons. (D) Single-cell extracellular recordings can be obtained concomitant with EEG recordings from one or several cortical and subcortical areas. *Abbreviations*: CPu, caudate putamen; LGP, lateral globus pallidus; SI, substantia innominata; HDB, horizontal limb of the diagonal band of Broca; AA, anterior amygdaloid area; ic, internal capsule.

A. Anesthesia

Several choices of anesthetics, including ketamine–xylazine, urethane, pentobarbital, are available. However, transport of the tracer during juxtacellular filling may depend on the activity of the cell being labeled. Therefore, for recording and labeling experiments barbiturate anesthetics may not be a good choice, since they are known to generally suppress neuronal activity (Richards, 1972). On the other hand, ketamine–xylazine, which is preferred for survival surgeries, may result in significant fluctuations in anesthetic plane in long recording experiments, in which variations in absorption may also result in relatively unpredictable redosing schedules. Urethane (ethyl carbamate) is our preferred choice for recording experiments because it appears to have little effect on neural activity, and its primary inhibitory actions seem to be restricted to some small neurons in the reticular formation (Rogers *et al.*, 1980). These examples make it clear that choices of anesthetic and other details depend on the particulars of the investigation. Discussion of the effects of different anesthetics on the firing properties of neurons is beyond the scope of this chapter. For additional details regarding anesthesia and surgical procedures, see theAppendix.

B. Choice of Juxtacellular Labeling Markers and Recording Solutions

The most logical choice of solution for juxtacellular labeling is one whose ionic composition is compatible with general extracellular recordings with the addition of biocytin [N_ε(+)-biotinyl-L-lysine, FW 372.5 g/mol; Sigma-Aldrich Co., St. Louis, MO] or Neurobiotin^{TM} (*N*-(2-aminoethyl) biotinamide hydrochloride, FW 322.85 g/mol; Vector Laboratories Inc., Burlingame, CA). The usual recording solution concentration ranges from 0.5 to about 1 M NaCl and contains 0.5–5.0% biocytin or Neurobiotin.

Difficulty to dissolve biocytin, especially when used in higher concentrations, is sometimes reported. This may be easily resolved by warming up the solution, strong agitation, sonication, or any combination of these. Dissolving biocytin in water and then mixing it with the NaCl solution may help. In addition, we have performed recordings and juxtacellular labeling using typical K-based solutions at concentrations usually used in intracellular recordings. In these cases, we did not notice any particular advantage or disadvantage for the labeling procedure. In general, all these solutions can be stored for several weeks at 4°C or for several months at less than 0°C.

The use of compounds other than HRP, biocytin, or Neurobiotin for juxtacellular labeling is theoretically possible, but we are not aware of any particular studies trying other substances. We have tried using biotin dextran amine [BDA(s), Molecular Probes, Eugene, OR] compounds, but the results obtained so far are inconclusive. Therefore, the tracers of choice for juxtacellular labeling are biocytin and Neurobiotin. In our hands, both provide very similar results, a finding that is in agreement with studies comparing

biocytin and Neurobiotin for intracellular labeling (Kita and Armstrong, 1991). According to Vector Labs, however, compared to biocytin and other neuronal labels, Neurobiotin is more soluble, iontophoreses better, and remains longer in cells. Neurobiotin also seems to be easier to dissolve than biocytin when used at higher concentrations.

Whether or not the solution needs to be filtered depends on how well the tracer is dissolved. If the solution appears completely crystal clear to the naked eye, it may not need to be filtered. Although filtering does not seem to have any adverse consequences. Because of the very small amounts of solution usually prepared (in the order of a few hundred microliters), it is advantageous to use very small filters, so that one loses the least amount of solution when filtering. Although any filter will do, the Cameo, 3 mm–0.22 μm acetate syringe filters, or the like are very effective.

C. Electrodes and Recording Apparatus

1. Single Unit Extracellular and Labeling Electrode/Glass

Microelectrodes are pulled from glass capillaries. Usually, 1.0–2.0 mm capillaries containing a microfilament fused to the inner wall are convenient choices because of their strength and commercial availability. The microfilament is very useful because it facilitates filling of the electrode and makes the filling more uniform, which minimizes trapped air bubbles. If there are air bubbles trapped in the solution (they are easily seen under the microscope), it is best to remove them. This can be done by gently tapping on the electrode while holding it vertically. In the worse case, bubbles can be removed by introducing a very thin wire into the solution in the electrode so as to make the bubble(s) attach to it; once attached to the wire they can be pulled out. This is done under the microscope with the electrode placed horizontally, usually glued to a glass slide with a small piece of putty.

A tungsten wire with a small enough diameter can be prepared for this purpose by thinning it in a caustic solution. First, attach the positive pole, for instance that of a 9-V battery, to the wire and the negative pole to a carbon rod. Fill a small beaker with caustic solution, introduce the carbon rod into it, and then slowly introduce the tungsten wire into the solution. The current passed will "eat up" the wire, thinning it. After rinsing it in water, this wire can be used for removing bubbles.

One easy way to fill an electrode with solution is by first placing a drop of solution on its back and waiting for a couple of minutes for the tip to be filled by capillary action, and then the rest of the electrode can be filled (from the back) by using, for instance, a micropipette filling needle. Some convenient choices for micropipette filling needles are the MicroFil™ ones sold by WPI (World Precision Instruments, Sarasota, FL).

Of several pullers available, the Narishige PE-2 (Narishige, Tokyo, Japan) vertical puller has been a common choice, perhaps because it is an older

model, which has been around for many years and is available in many laboratories. However, any puller able to handle the right size of glass capillaries will do. The tip of the electrode is broken under a microscope to a diameter in the range of 0.2–2.0 μm. The smaller the tip, the higher the impedance of the electrode. High impedance results in the detection of fewer neurons, but has the advantage that they are more likely detected only at a closer range. Therefore, higher impedance electrodes are more selective as the possibility of detecting more than one cell is diminished. Higher impedance electrodes should be used for detecting smaller cells whose electrical potentials are also smaller and need to be detected at closer ranges. In our experience, pipettes filled with saline and 2% biocytin, with tips of about 1–1.2 μm, have very convenient impedances of approximately 20–40 MΩ measured in the brain.

2. Extracellular Electrode/MUA/EEG/LFP/Metal

Electroencephalographic (EEG) or multiunit activity (MUA) and local field potential (LFP) data can be collected at the time a single cell is recorded. The advantage is that one can then correlate the extracellular activity of a single cell with the activity of a network. However, one should keep in mind that the characteristics of the EEG or LFP activity are highly dependent on the type and depth of anesthesia. Furthermore, the signals are also different in different brain regions and are significantly related to the cortical layer where the electrode tip is placed. Hence, the interpretation of the strength of the relationship or correlation of the single-cell activity and the network activity should take these and other factors (such as the distance between the two electrodes) into account. EEG and LFP can be collected with a host of metal electrodes (i.e., stainless steel, tungsten, etc.), most of which are easy to make and are also readily commercially available in bipolar and monopolar choices. Good ready-to-use metal electrodes can be purchased from Frederick Haer & Co. (FHC, Bowdoinham, ME). If one prefers to make them, appropriate wire can be purchased from California Fine Wire (CFW, Grover Beach, CA). To make electrodes, the wire is cut to the desired length (usually 5–8 cm), taking care to keep the electrode straight. One or two millimeters of insulation is removed from one tip and a little bit more from the other tip, where an appropriate connector needs to be clipped or soldered. A full discussion of EEG and electrode construction is beyond the scope of this chapter and the reader should consult one of the many specialized papers on the subject.

3. Electrophysiological Recordings and Recording Apparatus

Both EEG and single unit signals can be simultaneously collected, amplified, filtered, and recorded using standard equipment. In our preparations, we have used a Neurodata IR-183 amplifier (Neurodata Instruments, New York, NY) to record and juxtacellularly label single cells. For convenience,

both single unit and EEG tracers are usually displayed simultaneously in an oscilloscope or computer monitor and recorded directly to a computer hard drive via an interface. Recordings on magnetic tape for secondary storage and/or offline analysis are also common. Software and hardware combinations, such as Spike 2.0 from Cambridge Electronic Design Limited (CED, Science Park, Cambridge, England), are excellent choices for the acquisition of data via multiple channels. As computer power increases and cost decreases, direct storage of data into hard drives and quick online analysis with versatility of options become common practice.

D. Juxtacellular Labeling

After the collection of sufficient extracellular electrophysiological data to permit characterization of the recorded cell, one can proceed with juxtacellular labeling.

1. Getting Close to the Cell

Before labeling is attempted, the electrode needs to be in very close apposition to the cell being recorded; this is why the technique is called "juxtacellular" labeling. As the investigator advances the electrode closer to the cell, the amplitude of the unit's signal increases. The electrode should be advanced slowly in small steps of 1 or 2 μm. A sudden and substantial increase in baseline noise, sometimes accompanied by a transient jump in DC level, indicates a good position where to start experimenting with the entrainment of the cell.

2. Application of Pulses and Entrainment of the Cell

At the point when a juxtacellular position has been reached, anodal pulses in the range of 1–10 nA are usually used to eject the dye from the micropipette. These current pulses cause a vigorous response from the cell called "entrainment." An entrained cell fires action potentials at a higher frequency than normally observed both in response to and during the depolarizing phase of the current pulses being applied. Sometimes the neuron will also fire one or several spikes during the negative phase of the pulse. If the firing rate increases substantially during both phases of the pulse, the neuron is usually at risk of being killed. At that point the electrode should be moved back a few micrometers and/or the intensity of the pulses should be decreased. The experimenter can modulate entrainment to be on and off so as to avoid cellular damage. Uncontrolled firing at very high frequencies and during both phases of the pulse usually precedes irreparable cellular damage especially in slower firing neurons. The labeling procedure then requires that the experimenter pay attention to any electrophysiological

change the neuron may undergo before and during labeling. Pulse intensity should be low at the start and slowly increased until the cell responds. If the cell does not respond, the electrode is moved closer and the procedure is repeated. Once the cell responds to the pulse, the position of the electrode and/or the intensity of the pulses may need to be adjusted to avoid cellular damage. If repeated attempts to engage a cellular response fail with anodal pulses, cathodal pulses can be attempted. Figure 7.2 illustrates the

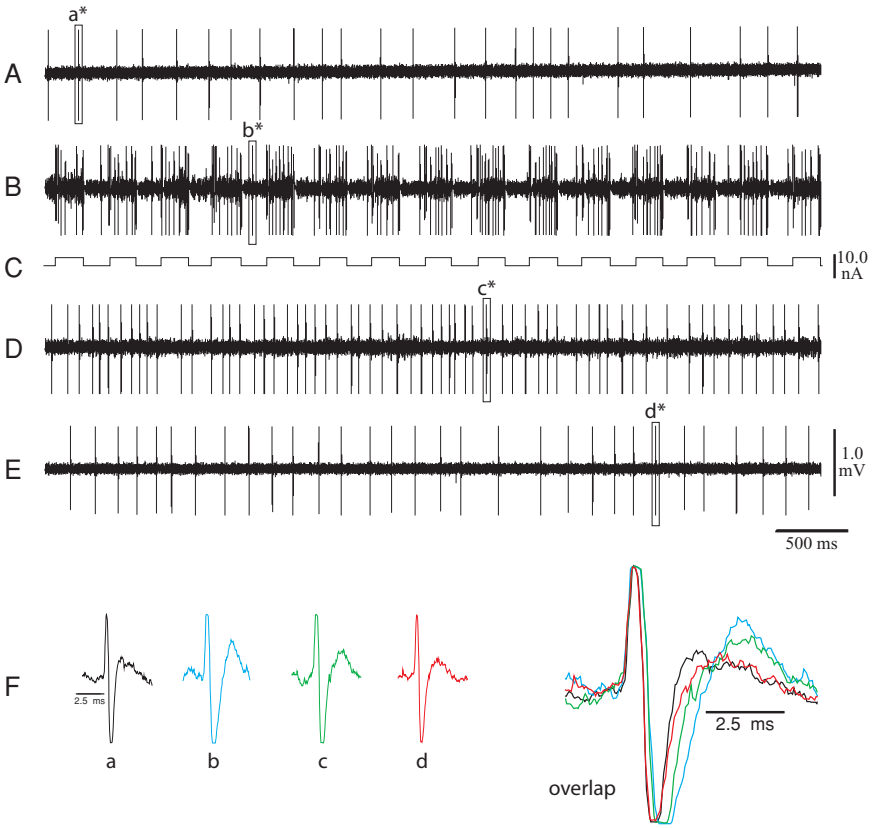

Figure 7.2. Extracellular recording and juxtacellular labeling protocol. Trace (A) shows the spontaneous firing of a neuron in the rat basal forebrain as recorded extracellularly. Trace (B) shows the entrainment of the neuron in response to the current pulses shown in trace (C). Notice that firing increases during the positive phase of the pulse but that the cell still fires spontaneously during some of the negative phases of the pulse (see b*). Also, notice that the base noise increased as compared to that in trace (A). Trace (D) shows that the spontaneous firing rate after cessation of the pulse is still higher than that before the entrainment, but with time (Trace E) it returns to preentrainment levels. Trace (F) shows selected extracellular action potentials before entrainment (a*), during entrainment (b*), and after entrainment (c*, d*). Their overlap illustrates how action potential width increases in a reversible manner during increased discharged frequency.

spontaneous firing of a neuron in the basal forebrain and its response to the current pulses.

The ability and the degree to which a neuron can increase firing rate probably depend on the neuron's molecular makeup and the state of the network where it resides. This is why some cells can entrain and fire at very high frequencies, while others cannot fire at such high frequencies in response to current pulses, although their firing rate still increases substantially, i.e., two- or threefold from their spontaneous rates. If the spontaneous firing rate is very low, say on the order of 1 Hz, then a sixfold increase should indeed be considered a very substantial change, despite the fact that a cell whose spontaneous firing rate increases just from 20 to 60 Hz appears to be more vigorously entrained. These vast differences that we have encountered in rat basal forebrain may be due to the diversity of cell types in this brain area. In particular, the compositions of their cellular membranes, ionic channels available, etc. in part dictate their very different intrinsic properties. Hence, it seems logical that they would respond in different ways to the same basic stimulus. Other important considerations arise, for instance, from geometrical constraints, the position of the electrode tip with respect to the soma, the shape and size of the soma, ephaptic relations, etc. In general, in our experience, faster firing neurons are much easier to label than slower firing ones, because they entrain easily and require less time for good quality labeling. Neurons whose firing rate cannot be modulated at all by the current pulse do not get labeled.

Generally, we applied pulses using an IR-183 Neurodata amplifier (Neurodata Instruments, New York, NY). Current pulses are 200 ms long (50% duty cycle). Entrainment for only a couple of minutes may be enough to label the soma. More complete staining of dendrites and axons requires in the order of at least 20 min.

3. Polarity of the Pulses

Both Neurobiotin and biocytin are zwitterions and should therefore be ejected from the micropipette with negative or positive current pulses. Pinault reported never to have seen labeling of neurons when applying iontophoretic negative (cathodal) pulses in the range of -50 nA to -1 μA (Pinault, 1996), an observation corroborated by others. However, in our own recordings and labeling of basal forebrain neurons, we have occasionally encountered cells that responded better, i.e., entrained better, in response to negative current pulses than to positive (anodal) current pulses. In these rare instances, the application of negative current pulses when using biocytin-filled electrodes did not result, as far as we could tell, in differences in the quality of labeling or required labeling time. Although these cells were not neurochemically identified, their morphology appeared similar to many other typical neurons of the basal forebrain. By chance, we did not attempt labeling of neurons by passing negative current pulses while using

Neurobiotin-filled electrodes. However, it is important to note that Kita and Armstrong (1991), although describing intracellular recordings and not juxtacellular labeling, reported that Neurobiotin is selectively ejected with positive current pulses. They also suggested that this property would be beneficial to electrophysiologists using hyperpolarizing currents to stabilize the membrane potential of neurons prior to recording.

4. Action Potential Shape and Cellular Response After Cessation of Pulse

To avoid false expectations of labeling, it is essential to make sure that the cell does indeed respond to the current pulses. If there is no response, the neuron will not get labeled. It is also important to corroborate that the neuron is still firing after cessation of the current pulse protocol and that it continues to fire as the electrode is slowly removed from its vicinity. The width of the action potential can be used to assess the health of a neuron and also serves to indicate that labeling has happened. In response to the current pulses, extracellular potentials can and usually become wider as shown in Fig. 7.2. Apparently this broadening indicates some micropuncture of the cellular membrane, a likely mechanism for the labeling (Pinault, 1996). After some time, extracellular action potential width does return to the level before injection, a possible indication of healing of the membrane. Also, it is likely that the firing rate of the neuron will be higher after cessation of the current pulse. However, over time it should return to baseline levels (Fig. 7.2).

E. Control Experiments: The Neuron Recorded is the One Labeled

In order to establish that the labeled neuron was indeed the neuron that was recorded, we designed several control experiments, some of them illustrated in Fig. 7.3. First, we applied current pulses 1–10 nA in intensity, for 15–30 min, without having first detected firing from a single neuron. This protocol resulted in no labeling of cells but if applied longer than approximately 20 min, it usually left a small accumulation of residual tracer in the tissue. Second, we applied current pulses of the same intensity for the same period of time as in the previous case, in the presence of a single unit, but without obtaining any response (entrainment) from the cell being detected. This protocol also resulted in no labeling of neurons. Third, we applied the same protocol while detecting a single unit and got the single unit to respond to the pulses. In this case a single-labeled neuron was later revealed and the morphological integrity of the neuron was preserved (Fig. 7.3A, B). Fourth, we labeled a neuron but killed it at the end of the labeling procedure by passing a high-voltage pulse. In these cases, when animals were perfused within approximately 1 h after the procedure, we indeed found a labeled neuron but usually its morphological integrity was

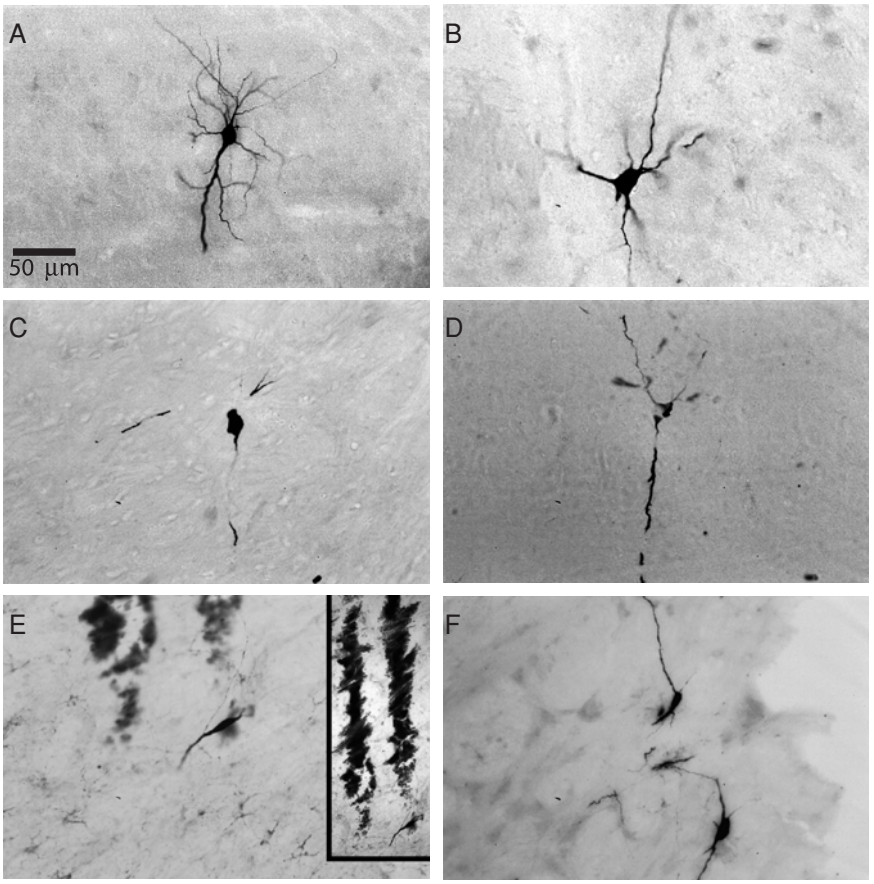

Figure 7.3. Control experiments: the neuron labeled is the one recorded. Delivery of current pulses without detection of a neuron or even when detecting a neuron that does not entrain results in no labeling of cells. (A) and (B) illustrate cases in which a single neuron was detected, recorded, and entrained (cells in two different animals). In each case, after juxtacellular labeling the electrode was retracted slowly while the cell was still firing. After proper histochemical procedures, a single-labeled cell was found. (C) and (D) illustrate cases in which after juxtacellular labeling of a single cell the neuron was "killed" by passing a high-voltage pulse. After histochemical procedures, a badly damaged single-labeled neuron was found in each case. (E) illustrates a case in which a single neuron was juxtacellularly labeled. The electrode was retracted dorsally until the cell was no longer responding to the pulses, yet these were passed for several minutes to create enough damage to mark the electrode track. Afterward, the electrode was totally removed from the brain and lowered again to the same depth at 75 µm lateral to the labeled cell, and pulses were passed again to mark a second electrode track (without detecting and entraining any other cells). After histochemical processing, one single-labeled cell was found at the end of a marked electrode track and 75 µm lateral to it, a second electrode track was found. (F) illustrates a case in which two neurons were detected and both responded (entrained) in response to current pulses. In that case, two labeled neurons were later found.

seriously compromised (Fig. 7.3C, D). If the animal was not perfused soon after the end of the procedure, the remains of the labeled cell sometimes were not found. Fifth, when we entrained a neuron for approximately 10 min. and then moved the electrode some micrometers away and proceeded to apply current pulses for another 20 or 30 min, without detecting and entraining a new cell or affecting the previously recorded neuron, we later found a single-labeled neuron and, most of the time, a single electrode track in the vicinity. Sixth, if by the same token, we first labeled a neuron for a few minutes, then retracted the electrode dorsally until the cell was no longer detected, marked the electrode track, and then removed the electrode completely out of the brain and moved it precisely, for instance, 75 μm laterally and returned the electrode to the same depth and proceeded to mark a second track, we later found a single track at the end of which we had a labeled neuron, together with a second track located laterally to the first 75 μm from it (Fig. 7.3E). Finally, if a single cell was entrained properly for labeling and then we still sporadically entrained a second neuron in the vicinity that was detected in the background, later we found a single strongly labeled neuron and a second weakly labeled neuron. However, if this procedure was carried out for a long time (i.e., 45 min), both neurons might be stained equally well, and then one could not determine with certainty which one was related to the main signal (Fig. 7.3F).

F. Histology and 3D Light and Electron Microscopy Reconstructions

1. Histology and Immunohistochemistry

Histological and immunohistochemical procedures for visualization and study of single juxtacellularly label neurons are identical to those followed for intracellularly labeled neurons. In short, animals are usually perfused with saline followed by a fixative such as acrolein, paraformaldehyde, glutaraldehyde, or a combination of these. Picric acid, glucose, and other chemicals are sometimes used to improve the outcome of a particular procedure. Protocols, including incubation times and amounts of chemicals used, are the choice of the investigator (see example in the Appendix), and there is a host of different recipes available in the literature.

2. 3D Light Microscopy Reconstructions

Modeling and experimental studies suggest that neuronal morphology (dendritic and axonal branching pattern) and class-specific connectivity play an important role in shaping network function (see chapters by Ascoli *et al.* and Nadasdy *et al.* in this volume). Two-dimensional (2D) camera lucida tracings of neurons have been performed following Cajal but all the focus-axis information is lost and the only view possible is that of the

plane of sectioning. Another disadvantage of this technique is that the end product is a drawing; one cannot statistically summarize the drawing without somehow measuring it. Fortunately, recent technological advances allow the use of 3D computerized reconstructions to obtain precise numerical details about morphological characteristics and constraints for different neuronal populations. These quantitative methods are needed in order to be able to compare and contrast different types of neurons in a logical, mathematical form. Through mathematics, the biological constraints on the architectural nature of the brain and of its elements can be investigated. For instance, dendritic size, together with their extensions into specific spatial domains, can be an indirect measure of input density. Understanding at least some of the structural diversity of dendritic arbors, their orientation, and size can provide essential clues about their possible connections and hence, clues about the intricacies of dendritic function.

Axonal reconstructions of identified neurons, although more difficult than dendritic reconstructions, provide some clues as to whether the neuron is a projection neuron, a local interneuron, or both. En passant or terminal varicosities can be recorded during the light microscopical reconstructions. These data, together with available information on the number and type of neurons in the environment of the axonal arborizing space, can be used for deriving the connectional probability of the electrophysiologically identified neurons (Zaborszky *et al.*, 2002). It is likely that digital experiments will be increasingly used with the advance of 3D cellular databases equipped with proper warping tools for data integration (http://www.ratbrain.org; see also chapter by Nadasdy *et al.* inthis volume). The data from these "in silico" experiments can be used to generate hypotheses that in turn can be tested in actual experiments. For the state-of-the-art stereological assessment of neural connections, see the chapter by Avendano in this volume.

Typically, dendritic and axonal trees can be reconstructed from serial sections using computerized microscope systems. The most widely adopted commercial system is the Neurolucida® system (MicroBrightField Inc.; www.microbrightfield.com), which utilizes a computer-controlled stepping motor stage and a high-resolution miniature CRT monitor. The motorized stage allows data acquisition to extend distances significantly larger than a single microscope field of view. The miniature CRT is coupled with the camera lucida and superimposes a computer graphic display on the actual image of the microscopic specimen viewed through the oculars of the microscope. This permits the acquisition of microscopic data that require high resolution and clarity to visualize. Neurolucida® is operated on a PC equipped with the Microsoft Windows operating system. Digital reconstruction of single-labeled neurons as well as analysis of the morphological data using the Neurolucida software suite (Glaser and Glaser, 1990) as well as other software tools for extracting morphomertic measurements from the reconstructed neurons are described in detail in the chapter of Ascoli and Scorcioni (in this volume). Neurons in the Neurolucida® system are represented by the x, y, and z coordinates of manually traced points; thus morphological

reconstruction is a very time-consuming process. There are other somewhat faster, but perhaps less precise, ways to combine traditional paper–pencil tracings with computer-assisted reconstructions of scanned images (see Ascoli and Scorcioni, this volume). Section "Applications" gives further details on reconstruction and morphological analysis of electrophysiologically and chemically identified neurons.

3. Electron Microscopy-3D Reconstruction from Ultrathin Sections

Electron microscopy of ultrathin sections produces high-resolution 2D images of cellular profiles and allows identification of synapses. However, most of the three-dimensional structural information is lost, although it can be recovered from reconstructing serial thin sections. The advantages of 3D reconstruction from ultrathin sections are several, including the ability to monitor plastic changes in the postsynaptic profiles (see chapter of Goldberg *et al.*, this volume), to better understand the complex organization of the neuropil, and to count synapses. Although the number of synapses can be deduced from 2D images using various correction factors or applying "unbiased" sampling strategies with optical dissectors as described in the chapter of Avendano in this volume, estimates of synapses can also be done from proper light microscopic reconstructions and application of an adequate electron microscopical sampling strategy. Although alignment of sections can be done manually (see Goldberg *et al.*, this volume), misalignment between sections due to mechanical and optical distortion often necessitates the use of computer programs. At present, the most popular program for alignment of EM images is the *Reconstruct* (V1.03.2) tool developed by Harris and Fiala (www.synapses.mcg.edu; http://synapses.bu.edu/tools/download.htm). This program computes the alignment from three points identified by the user in each image. A program under development that computes the fitting position using pixel density values results in more accurate alignment (Simon *et al.*, 2005).

G. Tracer Techniques in Combination with Electrophysiological Recording and Juxtacellular Labeling

1. Choice of Retrograde and Anterograde Tracers

Retrograde and anterograde tracers may be applied to the brain as an additional step prior to the juxtacellular labeling of single cells. Here, only some comments are presented with specific reference to juxtacellular labeling and the reader is referred to appropriate chapters in this volume for additional details about the tracers (Lanciego and Wouterlood, Reiner and Honig; Sesack *et al.*; and Wouterlood).

All tracer injections require animal survival to allow tracer transport from the injection site to the target area. It may be necessary to determine best

concentrations and survival times empirically. There are many excellent fluorescent tracers and selecting one depends on what fluorescent tag will be used for visualization of the single cell. If, for instance, rhodamine (red) is used for the visualization of the single cell, then a yellow or blue (or both) fluorescent retrograde/anterograde tracer is a convenient choice. Fluorogold (Fluorochrome Inc., Denver, CO) and Fast Blue (Sigma, St. Louis, MO) are primarily retrograde tracers. The fluorescent dextrans are commonly used as anterograde or retrograde tracers (Reiner and Honig, in this volume), and these include rhodamine isothiocyanate, rhodamine B dextran, lysinated tetramethylrhodamine dextran (Fluoro-Ruby), and Fluoro Emerald. Their advantages seem to be less diffusion at the injection site and more permanent labeling than with the corresponding free dyes (Schmued *et al.*, 1990; Schmued and Heimer, 1990; Schmued, 1994). BDAs can also be used as retrograde and anterograde tracers and offer superior characteristics and versatility (Reiner *et al.*, 2000). Since BDAs contain biotin, their use in combination with biocytin or Neurobiotin labeling may be tricky and is therefore not recommended. Other more direct choices of anterograde and retrograde compounds for fluorescent detection include True Blue, Granular Blue, 4′,6-diamidino-2-phenylindole, Diamidino Yellow, Nuclear Yellow, and Rhodamine Latex Beads, among others.

2. Sources of Artifact

There are several potential sources of artifact when tracers are injected into any part of the brain. Two particular problems are the size of the tracer uptake zone and the possibility of uptake of the tracer by fibers of passage at the injection site. To minimize the fibers of passage problem, the simplest rule is to minimize brain injury. To control the size of the tracer uptake zone, tracer injections need to be steady and slow (over 10–15 min), which in our experience creates less tissue damage and also minimizes the spread of the injection by avoiding stressing the tissue around the injection site. To avoid leakage of tracers along the pipette track, the exterior of the needle needs to be cleaned and dried before inserting into the brain and must be left in place for at least 5 min after the end of the injection. This technique appears to minimize damage to the tissue and also reduces the possible uptake of tracer by fibers of passage. However, the uptake of most tracers by fibers of passage cannot be entirely abolished. To minimize movement of the needle and improve reproducibility of injections, the syringe in use may be mounted on a Hamilton Chaney adapter. Also, many tracers may have a small component of transport in the opposite direction to the one intended, such as in the case of vestiges of retrograde transport for an otherwise mainly anterograde tracer injection or vice versa. In addition, because of the difficulty in limiting the injection exclusively to the area of interest, one strategy that can be used is to apply injections of different sizes (in different animals) so that larger injections can increase the chance of including the majority of the target area while smaller injections cover only portions of it.

III. APPLICATIONS

In this section we will illustrate the application of juxtacellular labeling of single neurons to the study of neural circuits of the basal forebrain of the rat. As outlined in Fig. 7.4 and illustrated in subsequent figures, we increase the level of complexity of the investigation of single basal forebrain neurons by increasing the number of procedures that are performed in addition to extracellular recording and juxtacellular labeling. These added procedures provide information about the transmitter, dendritic and axonal arborization pattern, and connectivity of single electrophysiologically identified neurons that could not otherwise be obtained, and which in the past has been only inferred from separate experiments. This multiplicity of methods is

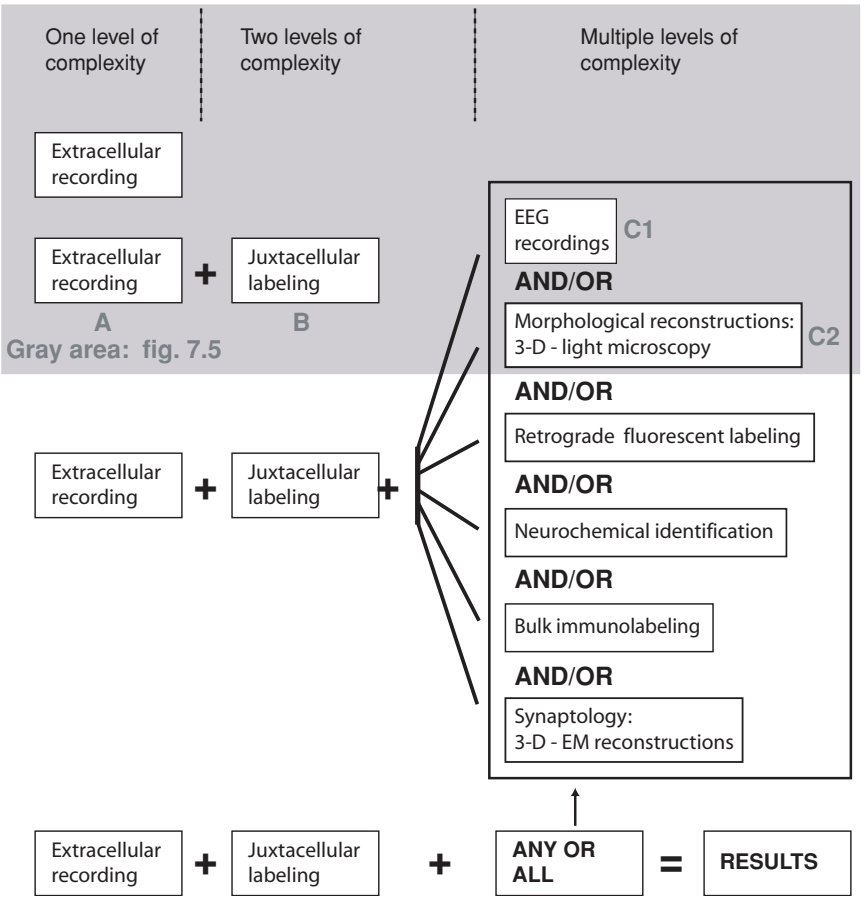

Figure 7.4. Schematic illustration of the general experimental strategy: extracellular recording and juxtacellular labeling of single neurons in combination with several methods that allow further cellular characterization. The added levels of complexity increase the amount of information collected about a single neuron. Letters A, B, C1, and C2 are illustrated in detail in Fig. 7.5.

necessary because simplified criteria, which in some brain areas have been successfully used to differentiate among different cell types, have failed in the basal forebrain due to the heterogeneity of electrophysiological, morphological, and neurochemical characteristics found in this region. This combination of techniques has allowed us to study the EEG correlation of the discharge properties of neurochemically and morphologically identified neurons in the basal forebrain (Duque *et al.*, 2000). Our studies, for instance, indicated that both cholinergic and parvalbumin-containing neurons increase firing during cortical low-voltage fast-electrical activity (LVFA), and therefore belong to the previously established category of "F" (fast) type basal forebrain neurons. On the other hand, neuropeptide Y positive (NPY) neurons that showed increased firing during cortical slow waves belong to the so-called S (slow) cell type. Whether or not this is the case for all basal forebrain cholinergic, parvalbumin, and NPY neurons is not known. Additional morphometric and synaptology studies in progress will allow us to build the "basic circuitries" of the basal forebrain that are critical to understand its functions.

A. Electrophysiological and Morphological Identification of Single Neurons

Figure 7.5 illustrates a typical experiment consisting of a single-cell extracellular recording with juxtacellular labeling and subsequent morphological reconstruction of the recorded neuron. This neuron was labeled for approximately 5 min by passing +8 nA current pulses.

From single-cell electrophysiological recordings, we classified this neuron as a bursty cell with a firing rate of 2.95 Hz. Its action potential shape is triphasic with a rise time of approximately 0.36 ms and total width of 2.88 ms. Labeling of the cell permitted us to locate the soma within the horizontal limb of the diagonal band of Broca. The soma measures 15 × 14 μm and its shape is round with six primary dendrites. The cell is a typical basal forebrain neuron according to a previous classification using the juxtacellular technique (Pang *et al.*, 1998). Panel C1 in Fig. 7.5 illustrates how one additional electrophysiological procedure, EEG, concomitant with the single-cell recording further allows the classification of this neuron into the "S" category of basal forebrain neurons. This categorization indicates that the firing rate increases during high-amplitude slow-cortical EEG activity and it is different from neurons that have a faster firing rate during fast cortical EEG activity, which were termed "F" cells (Detari and Vanderwolf, 1987; Dringenberg and Vanderwolf 1998; Detari, 2000). The simultaneous recording of EEG and single-cell electrophysiological data also revealed that there are neurons in the basal forebrain whose activities remain unchanged despite EEG cortical changes (Nunez, 1996).

Figure 7.5C2 illustrates how one additional procedure, 3D light microscopy reconstruction, further advances our knowledge of this single neuron. For instance, in addition to the soma shape and location, we now

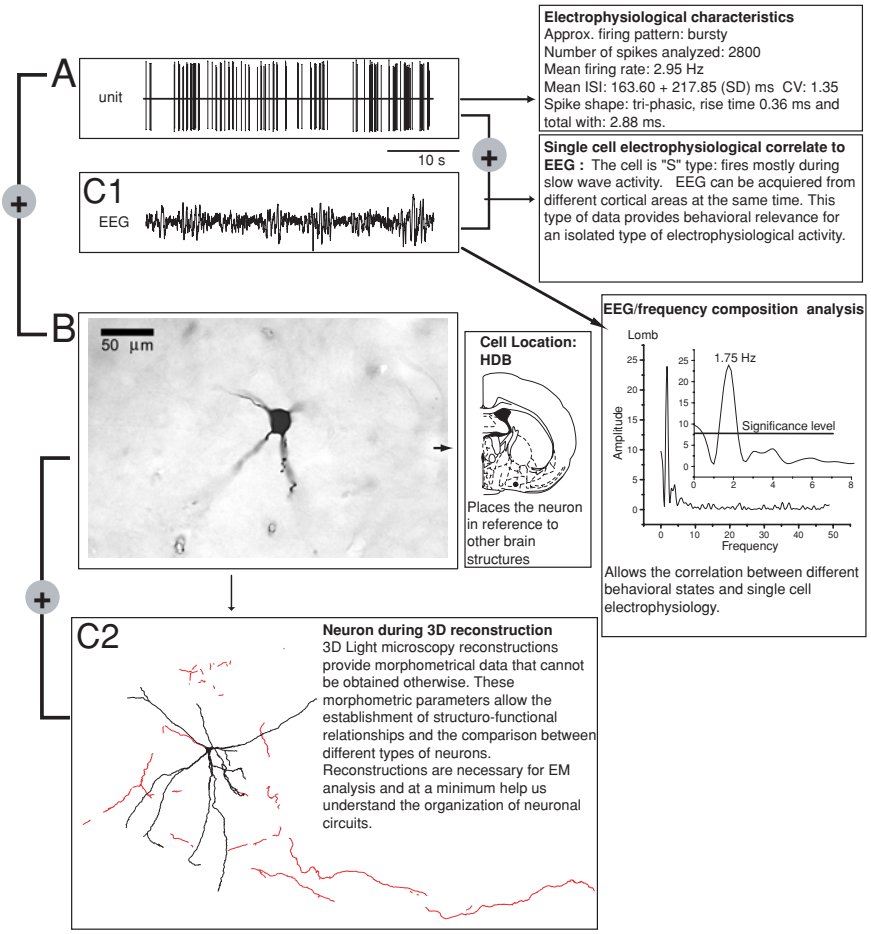

Figure 7.5. Example of extracellular recording and juxtacellular labeling in combination with EEG recording and morphological reconstruction. Arrows point to boxes containing examples of information that can be collected about the neuron from the different combined methods.

know the extent and direction of its dendritic tree. We know that the neuron has axon collaterals that communicate with nearby neurons and also a main projection axon that runs in the ventromedial direction. This extra information allows the formulation of hypotheses and the planning of further experiments. Do all "S" cells have axon collaterals? If so, what types of local neurons are contacted by "S" cells? Do they all have a projection axon?

B. Retrograde Labeling of Electrophysiologically Identified Neurons

Figure 7.6 illustrates the characterization of a basal forebrain neuron using an additional procedure to the ones illustrated in Fig. 7.5. In this case,

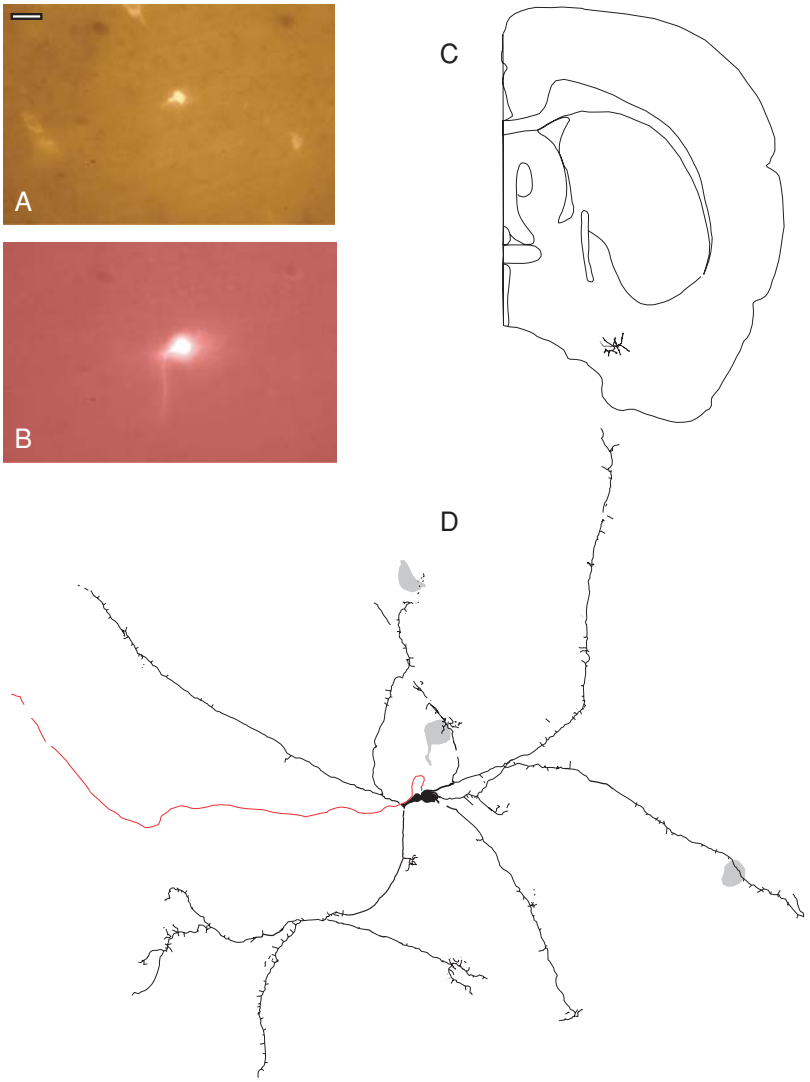

Figure 7.6. Juxtacellularly labeled ChAT negative, parvalbumin-negative basal forebrain corticopetal neuron. This neuron was not tested for NPY. (A) The cell is retrogradely labeled with Fluorogold from the prefrontal cortex. (B) The single biocytin-filled neuron visualized with avidin-conjugated rhodamine. (C) Coronal section illustrating the position of this cell. (D) Partial neurolucida reconstruction showing that this neuron has only one projection axon (in red) and no axon collaterals in the neighborhood. The gray spots represent cholinergic neurons in close proximity to some dendritic appendages. Scale bar in (A) (applies to B also): 50 μm.

approximately a week prior to the single-cell recording and juxtacellular labeling, the animal received an injection of the retrograde tracer Fluorogold into the prefrontal cortex. The biocytin-labeled neuron was first visualized with avidin-conjugated rhodamine (Fig. 7.6B). This neuron was retrogradely

labeled with Fluorogold (Fig. 7.6A), indicating that it projects to the prefrontal cortex. Additional immunostaining protocols revealed that this particular juxtacellularly stained and retrogradely labeled neuron was negative for both choline acetyltransferase (ChAT) and parvalbumin, markers for cholinergic and GABAergic neurons, respectively. After conversion of the rhodamine fluorescent signal (juxtacellular staining) to nickel-enhanced DAB, the tissue was processed for ChAT using DAB as end product. As the 3D light microscopy reconstruction shows (Fig 7.6D), there are three cholinergic cell bodies in the vicinity of this electrophysiologically identified and morphologically reconstructed cell. This identified neuron was F type and a "just" projection neuron, since only a single axon was found that lacked local collaterals. These extra procedures augmented the information collected about this single neuron. Now we know its single-cell electrophysiological characteristics and the correlation of these to the EEG (to the state of the animal). In addition, we know some of the transmitters or chemical markers for which it was negative, where it projects to, its morphology, and the important fact that it did not have axon collaterals.

C. Chemical Identification and Morphometry of Juxtacellularly Labeled Neurons

Figure 7.7 illustrates the addition of neurochemical identification to the characterization of a single basal forebrain neuron. In this case, the single neuron filled with biocytin was first visualized with avidin-conjugated rhodamine (Fig. 7.7C) and subsequently found to be positive for the calcium-binding protein parvalbumin, visualized with fluorescein isothiocyanate (FITC) (Fig. 7.7B). After conversion of the rhodamine fluorescent signal to nickel-enhanced DAB, the section containing the cell body of this electrophysiologically and chemically identified cell was immunolabeled for ChAT. As Fig. 7.7A shows, a cholinergic cell body (blue profile) was found in the vicinity of the reconstructed parvalbumin-positive neuron that seemed to be approached by axon collaterals of the electrophysiologically identified neuron.

Figure 7.8 displays some morphometric data regarding the dendritic tree of this parvalbumin-positive neuron, which had previously been electrophysiologically identified. Panel A in Fig. 7.8 is the dendrogram showing the dendritic tree of this neuron drawn in the same colors as used in the tracing of Fig. 7.7A. A dendrogram is a stylized drawing of a branched structure, e.g., axon or dendrite. The purpose of a dendrogram is to visualize the complexity of the 3D arborization pattern of the tree in a manner that can be easily compared among different neurons. This dendrogram shows that this particular parvalbumin neuron has eight dendritic trees, each dividing into several daughter branches with a total length of 8785 μm. The graph in Panel D, which displays the mean diameter of the dendritic branches, indicates that primary dendrites are thicker and that as dendritic order

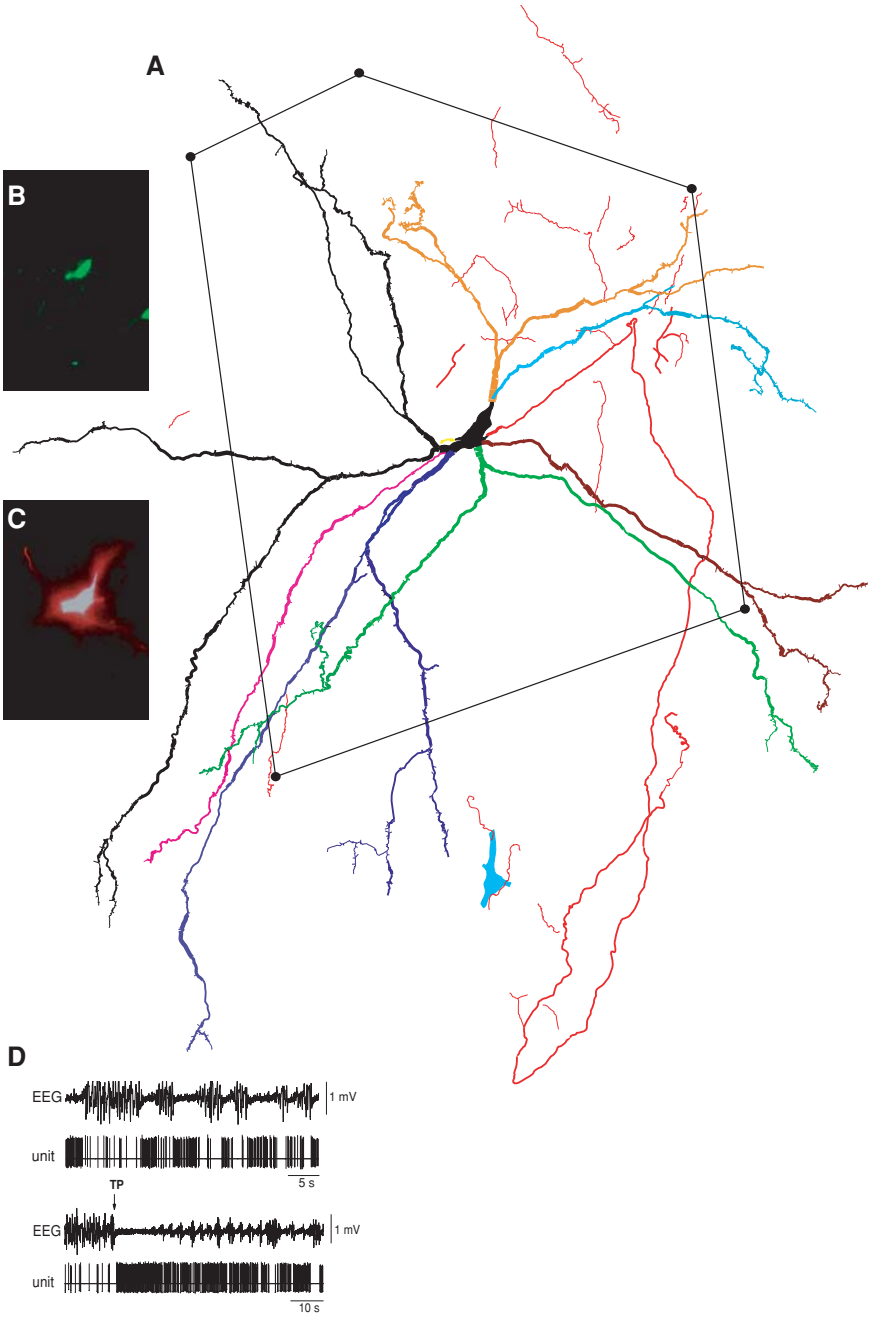

Figure 7.7. (A) Partial reconstruction of a juxtacellularly labeled basal forebrain parvalbumin-positive neuron. The axon is shown in red. The soma and one of the dendrites are shown in black and the other dendrites in different colors. Each dendrite matches its color in the dendrogram shown in Fig. 7.8A. The pentagon encloses pieces of the neuron that are found in one of the sections from the serial reconstruction and it corresponds to the block face shown in Fig. 7.9A. (B) The neuron stained for PV (FITC). (C) Biocytin-filled neuron visualized with rhodamine. (D) Concomitant unit and cortical EEG spontaneous and tail pinch (TP) induced activity.

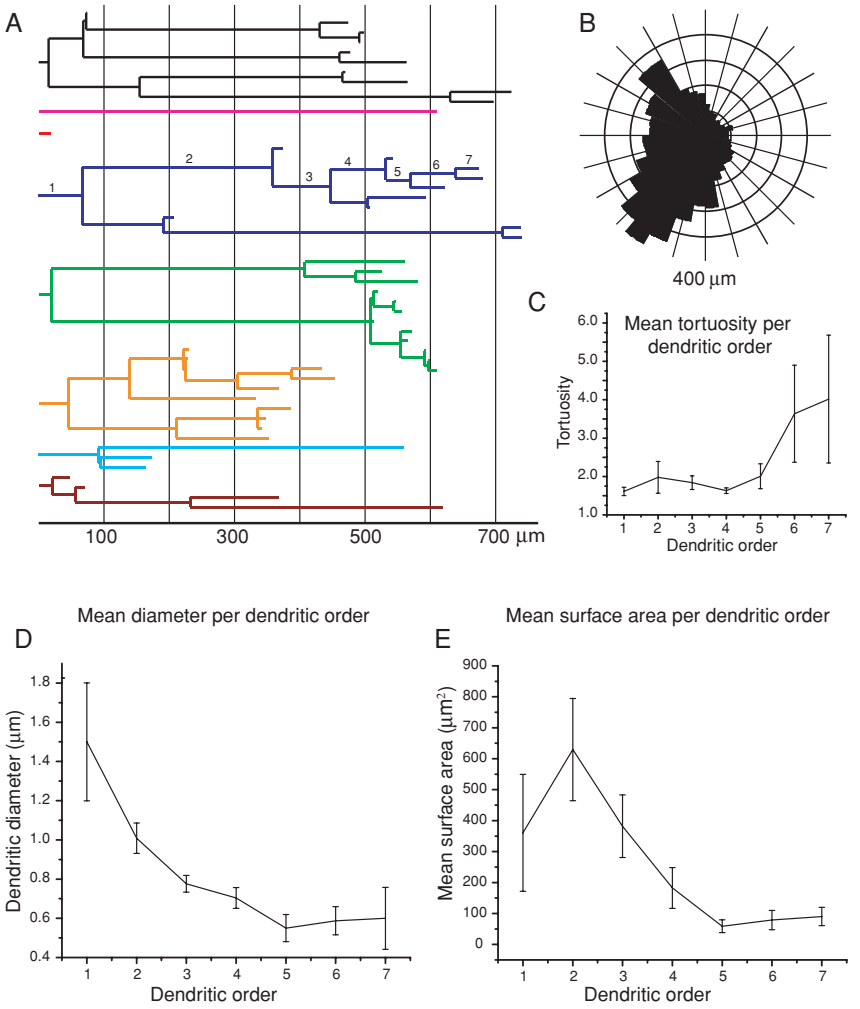

Figure 7.8. Corresponding dendrogram (A) and dendritic polar histogram (B) for the PV neuron shown in Fig. 7.7. The numbers at the abscissa in (A) represent length of the dendritic trees in micrometers. The various dendritic trees are colored the same way as in Fig. 7.7 to facilitate comparison. The outer circle of the polar histogram corresponds to a 400-µm diameter around the origin. C, D, and E illustrate mean tortuosity, mean diameter, and mean surface area all as functions of dendritic order, exemplifying different types of morphometric analyses that can be performed on data acquired with Neurolucida reconstructions. All error bars correspond to the SEM. For further explanation see text.

progresses dendritic branches become thinner, although the end portions of the dendrites have a tendency to be a bit thicker. This trend is similar to the situation observed in cholinergic neurons and is opposite to that in NPY neurons whose endings are very thin (Duque *et al.*, in preparation). The mean surface area, shown in Fig. 7.8E, is maximum in the case of secondary

dendrites and about the same between primary and tertiary dendrites. Since tertiary dendrites, which are thinner than secondary and primary branches, have as much surface area as primary dendrites, it is reasonable to deduce that tertiary dendrites are longer than primary and secondary dendrites, which is indeed the case (not shown). Higher order dendrites have overall much less surface area. This type of analysis helps make predictions as to what to expect in terms of numbers of inputs, i.e., primary and tertiary dendrites could get roughly the same number of inputs, but second-order dendrites might get more inputs since they have on average more surface area. The polar histogram shown in Panel B gives a characterization of the directional distribution of dendritic growth projected onto the plane of sectioning, similar to the analysis described by McMullen and Glaser (1988). The algorithm for polar histograms breaks up the dendritic processes into line segments and determines the directions in which these line segments point and their corresponding lengths. The direction of the vector is calculated by projecting the line segment onto the plane of sectioning. The histogram represents total length by the distance from the origin and the angle that the vector makes with the *x*-axis plotted in the radial direction. Each sector in the polar histogram is the sum of all the dendritic growth in that particular range of angle. The dendrogram is another tool to compare quantitatively different neurons. The dendritic tortuosity displayed in Panel C gives a ratio between the actual length of a dendritic segment and the distance between its endpoints. Both the tortuosity and the dendritic orientation, as measured with the polar histogram, can determine spatial correlation between overlapping axonal and dendritic arbors, thus affecting the probability of connections (see also Zaborszky *et al.*, 2002; Stepanyants *et al.*, 2004). These analytical tools are provided in the Neurolucida software package. Additional analyses that would also permit elaborate comparison of dendritic morphometric parameters between various neuronal types (Scorcioni *et al.*, 2004; Li *et al.*, 2005) can be performed using *L-Measure* (Scorcioni and Ascoli, this volume), a JAVA program freely available both for download and for Web-based usage (http://www.krasnow.gmu.edu/L-Neuron).

D. Synaptology of Electrophysiologically and Chemically Identified Neurons

Embedding tissue sections containing electrophysiologically and chemically identified neurons into plastic allows the study of the different neurons' synaptic relationships. For example, we can study the input to specific dendritic compartments of an electrophysiologically and chemically identified neuron. Figure 7.9 shows the intermediary documentation, at the LM level, for a small dendritic segment of the parvalbumin neuron depicted in Fig. 7.7. Figures 7.10 and 7.11 show various boutons that impinge on the dendritic shaft of this parvalbumin neuron. Figure 7.12 shows a 3D rendering of the same piece of dendrite reconstructed from 66 ultrathin sections. As

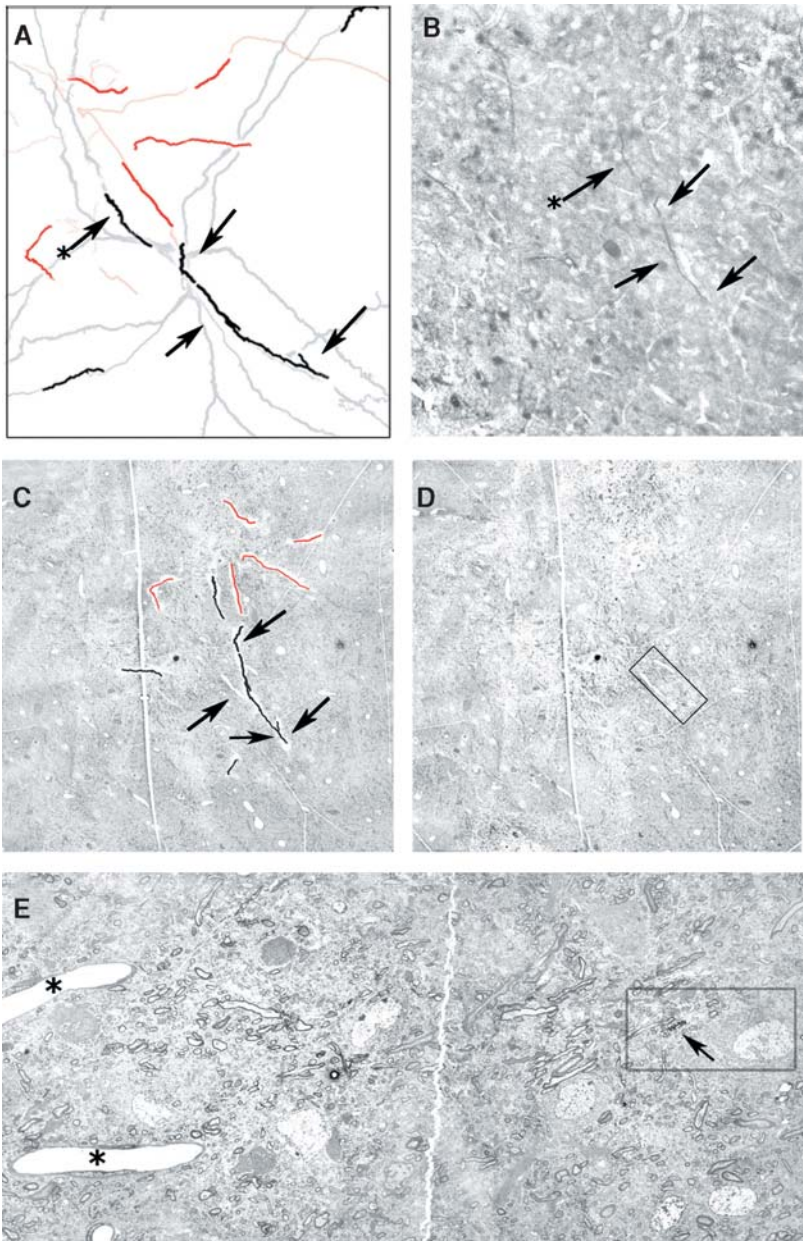

Figure 7.9. Correlated light–electron microscopy of the parvalbumin neuron shown in Fig. 7.7A. (A) Processes of this neuron contained in section 17 that was serially thin sectioned are shown against the full arborization of this neuron displayed as background. (Compare this panel with the enclosed processes in the pentagon of Fig. 7.7A). Axons are in red and dendritic processes are in black. (B) Blockface image of thick section 17. Three arrows point to a dendritic shaft that is also labeled in (A). Arrow with asterisk points to another dendritic shaft to facilitate comparison. (C, D) Low-magnification (190×) montage of a thin section from this material with

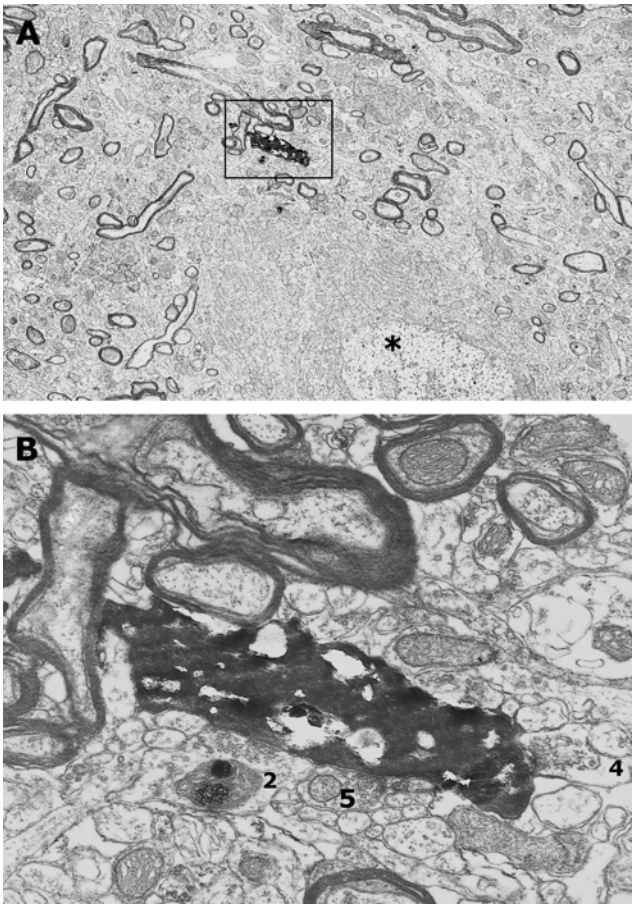

Figure 7.10. (A) Low-magnification electron micrograph (1400×) to show the boxed area from Fig. 7.9E. (B) High-power electron micrograph to illustrate the dendritic segment that has been 3D reconstructed from serial thin sections. Numbers denote different boutons.

the 3D model shows, this dendritic segment, which is about 3 μm in length, is surrounded by 11 boutons and most of them had synaptic appositions. Knowing that the total length of the dendrites of this parvalbumin neuron is 8785 μm, one can estimate that this neuron may receive as many as

←

Figure 7.9. (*Cont.*) (C) and without (D) processes as seen in the Neurolucida file (A). The boxed area in (D) is enlarged in (E). (E) Low-power electron micrograph (440×) showing the boxed area from (D). The boxed area in (E) is shown at higher magnification in Fig. 7.10A. The two capillaries with asterisks are fiducial markers to compare (D) and (E). Arrow in the boxed area points to the small dendritic piece that is displayed in higher magnification in Figs. 7.10–7.11 and in the 3D model of Fig. 7.12.

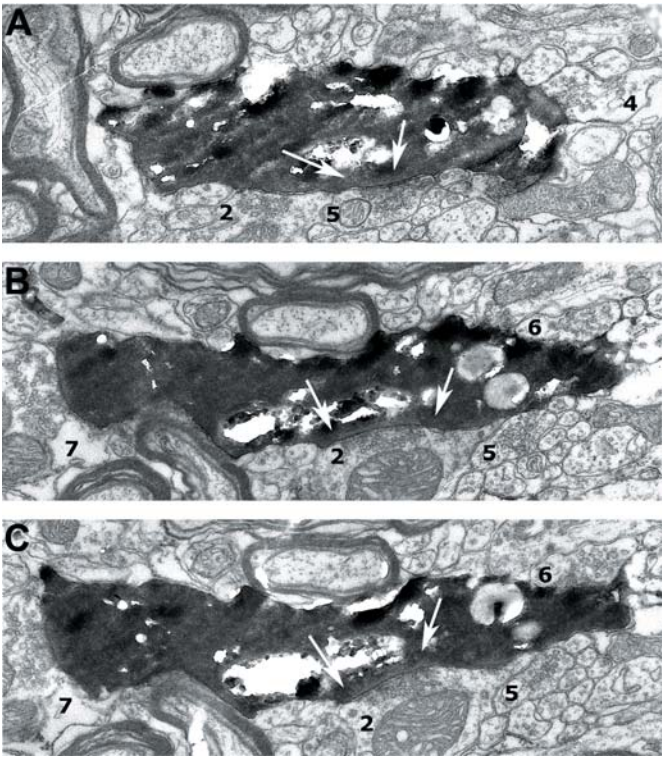

Figure 7.11. (A) Ultrathin section 23 in which boutons 2, 4, and 5 can be recognized (compare Fig. 7.10B). (B) and (C) show ultrathin sections 24 and 26 from the series of 66 sections with additional boutons 6 and 7. White arrows point to synaptic attachments.

32,000 synapses. However, since primary, secondary, etc. dendritic branches possess different diameters and may be contacted by different axons, for a more accurate estimation one has to select samples from each dendritic segment and the terminal branches of the dendritic trees. The dendrogram depicted in Fig. 7.8A helps to design the sampling strategy. As discussed under section "Chemical Identification and Morphometry of Juxtacellularly Labeled Neurons." dendritic length, diameter, and surface area values can affect the spatial arrangement of incoming boutons. In addition, analyses on electron micrographs (e.g., average bouton size) and data from tracing studies need to be taken into consideration if we want to arrive at a realistic estimation of the type and synaptic number than can impinge on single or statistically derived average neuron (Zaborszky *et al.*, 1975). Similar morphometric analyses on the axonal tree in conjunction with available data on the number of neurons that are in the space of axonal arborizations can help to estimate the number and postsynaptic targets of the local axon collaterals of electrophysiologically identified neurons (see Zaborszky and Duque, 2000).

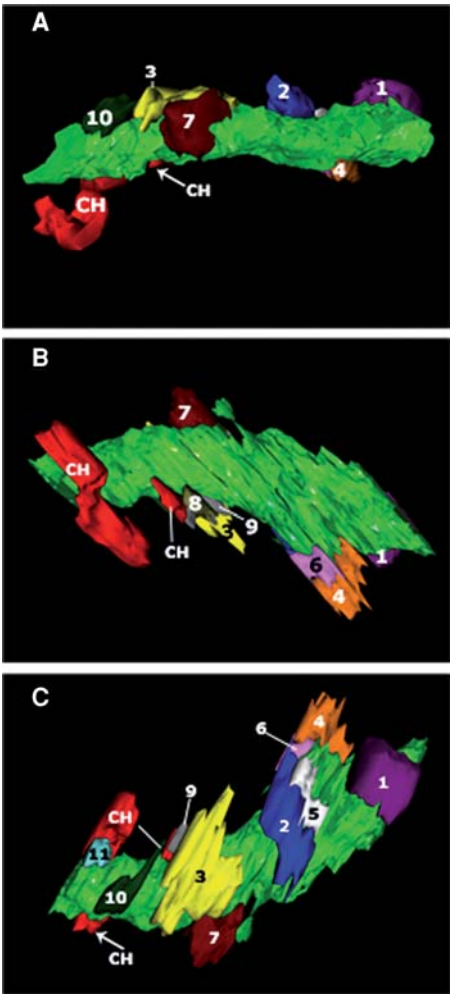

Figure 7.12. 3D partial reconstruction of the dendritic segment of the parvalbumin neuron illustrated in Fig. 7.7A. This 3D model consists of 66 ultrathin sections, rotated along the dendrite (green color). Numbered boutons are labeled with different color. Boutons labeled with numbers 2, 4, and 5 can also be seen in Figs. 7.9B and 7.10B. Boutons 2, 5, 6, and 7 can be identified on Fig. 7.11B, C. The red surface marked with CH corresponds to cholinergic dendritic profiles that are in close vicinity to the parvalbumin dendrite.

IV. SUMMARY OF ADVANTAGES AND LIMITATIONS

The fundamental advantage of any single-cell recording technique combined with the labeling of the recorded cell is that it allows the correlation of physiology and morphology at the cellular level. The advantage of juxtacellular labeling is its compatibility with a host of other techniques that, when combined, advance our ability to characterize single neurons in many

different ways. By virtue of being extracellular, the recording can usually be maintained for prolong periods of time and it is less prone to disruptions due to movement. Hence, recording and labeling of neurons can be done both in superficial, i.e., cortical, as well as in subcortical structures that are several millimeters deep. Juxtacellular labeling allows for the staining of neurons in deep subcortical structures with a success rate of usually more than 80%. Neurons labeled with biocytin or Neurobiotin can be stained for light microscopy and/or electron microscopy using chromogens such as DAB. Juxtacellular labeling of single neurons is compatible with immunohistochemical techniques, making it possible to collect data about the chemical identity of the recorded and labeled cell. As seen in the previous examples, these advantages do not sacrifice the possibility of fine morphological evaluation at the light and/or the electron microscopy levels.

The staining obtained with juxtacellular labeling can reach Golgi-like quality in the soma and dendrites. It seems that myelinated axons are always filled. However, depending on labeling time and quality of entrainment, some axons are not fully labeled.

A. Advantages

1. The stability of the method allows long recordings, which in turn permit more complete electrophysiological characterizations.
2. The method allows for recording and successful labeling of neurons in various brain structures, particularly in very deep subcortical regions, where intracellular recordings are almost impossible to obtain.
3. At least in theory, the natural cellular membrane and intracellular environment is less disturbed since the cell is not being impaled with an electrode.
4. The method is species independent and compatible with immunohistochemistry and electron microscopy.

B. Limitations

1. Because the recording is extracellular, postsynaptic potentials cannot be recorded.
2. Quality of the "fill" depends on the length of time the cell is entrained and might not be as complete as the filling with intracellular techniques if the cell is not labeled long enough.
3. Axonal labeling may also be partial, but this again seems to depend on labeling time.
4. Occasionally, a glial cell in the vicinity of the labeled cell may also get labeled.
5. The combination of juxtacellular labeling with many other techniques, although powerful in providing exquisitely detailed characterization of single cells, can be limited in practice because it is labor-intensive and time-consuming.

APPENDIX

As illustrated in Fig. 7.4 and throughout examples in section "Applications", the advantage of juxtacellular labeling is its compatibility with many other techniques, which allows increasingly detailed characterization of a single cell. Figures 7.6–7.12 give an outline of possible steps for a sample experiment in which a neuron can be retrogradely labeled and then tested for several neurochemicals to be then converted to Ni-DAB, double labeled for ChAT bulk immunostaining, reconstructed, and finally analyzed at the EM level.

A. Animal Preparation Prior to Electrophysiological Recordings

Day 0

1. *Anesthesia*: Because these are survival surgeries, use a mixture of ketamine (85 mg/kg) and xylazine (15 mg/kg) i.p. Do not use urethane, as it affects gastrointestinal motility (Yuasa and Watanabe, 1994) and is toxic to the liver and lungs (Renuka and Dani, 1983). Do not use pentobarbital; it may affect retrograde and anterograde tracer transport (Rogers *et al.*, 1980). Gas anesthesia can also be used.
2. *Stereotaxis*: For stability and proper location of brain structures, anesthetized animals need to be placed correctly in an appropriate stereotaxic apparatus. Wound margins and points of contact between animal and stereotaxic apparatus are usually infiltrated with lidocaine solution (2%) and xylocaine ointment (5%), respectively. Aseptic conditions are necessary.
3. *Tracer injections*: Fluorogold is primarily a retrograde tracer. Prepare it at 2.5–4% in double distilled H_2O. Pressure inject 0.05–0.3 μl/10 min/per site using a 1 μl Hamilton syringe. Survival time: 2–14 days. Fast Blue (FB, Sigma): same as for FG.

B. Animal Preparation for Electrophysiology

Day 1

1. *Anesthesia*: Use urethane 1.3 g/kg i.p. Usually injected once. Caution: Urethane is highly toxic.
2. *Surgery*: Place animal in a stereotaxic apparatus as described before. Retract scalp and overlying fascia from the skull and puncture the atlanto-occipital membrane to allow drainage of some cerebral spinal fluid. Keep body temperature at 37–38°C preferably with a hot water circulating pad. Drill small burr holes in both hemispheres, over, for instance, the frontal cortex for EEG recordings [anteroposterior (AP) +1.6–1.8 mm, mediolateral (ML) ± 0.5–2.0, relative to bregma] and

over the basal forebrain (AP −0.3 to −1.0), L ±2.4–3.2 mm, relative to bregma) for single unit recordings.

C. Electrophysiology and Labeling

1. *Electrode fabrication*: Make recording microelectrodes from 2.0 mm outer diameter borosilicate glass capillaries (World Precision Instruments, Sarasota, FL) on a Narishige PE-2 vertical pipette puller. Break the tip of the electrode under visual guidance to approximately 1.0 μm in diameter. Fill the electrode with 0.5 M NaCl containing 4% biocytin. Measure in vitro impedance and use 10–30 MΩ electrodes.
2. *Set up EEG electrodes and obtain a signal*: Find and record a neuron long enough to allow statistical significance test to be performed for its single-unit electrophysiological characterization. Record EEG and single-cell electrophysiology at the same time, to allow correlation analysis.
3. *Labeling*: Get as close as possible to the cell. Entrain the cell by passing current pulses 1–10 nA in intensity. Monitor entrainment and move the electrode closer to or further away from the cell or increase or decrease pulse intensity as necessary to maintain entrainment without causing cellular damage. Entrain cell for at least 20 min to obtain good labeling.

D. Perfusion

Within a few hours after the termination of the labeling protocol, perfuse the animal transcardially.

Pass 100 ml normal saline followed by 200 ml of ice-cold fixative [4% paraformaldehyde, 15% saturated picric acid, and 0.05% glutaraldehyde in 0.15 M phosphate buffer (PB), pH 7.4], followed by 200 ml of the same fixative without glutaraldehyde.

Remove brain and postfix at 4°C overnight in the fixative without glutaraldehyde.

Optional: Cryoprotect in sucrose if the brain is to be cut frozen in a cryostat or on a freezing microtome.

E. Cutting and Pretreatment of Sections

Day 2

1. *Cutting*: Dissect the block of tissue containing the cell. The size of the block depends on what you expect and want to process. If long projection axons are expected, then cut the block so that it contains the area with the terminals of the axon. Notch one side of the brain so that you

can keep track of left and right hemispheres. Cut coronal or sagittal sections 50–60 μm thick with a Vibratome® or freezing microtome if only light microscopic processing is planned.

2. *Rinsing*: Select the sections to be processed and rinse them several times in cold PB until the yellowish color of the picric acid disappears. All rinses from here on should be done in cold 0.1 M PBS. Every rinse should take about 5 min, while gently agitating the sections in a shaker.
3. *Borohydride and peroxidase pretreatments*: Incubate sections in 1% sodium borohydride in PBS (to remove excess aldehydes) for 20 min. Rinse 3–5 times or until the bubbles are gone and the sections sink. Then incubate for 10 min in 1% hydrogen peroxide in cold PBS (to block peroxidases) and rinse again three times.

F. Visualization of Biocytin-Filled Neuron and Digital Photography

Days 3 and 4

1. Select 48 sections where you expect to find the soma of the juxtacellularly labeled neuron (so that the soma will be found within 2.4 mm of tissue, which is considered a very large margin of error). Store the rest of the sections in PBS at 4°C.
2. Incubate the sections overnight (4°C, in a shaker) in avidin-conjugated rhodamine (R) (1:500; Jackson ImmunoResearch Labs, West Grove, PA). This can be done in six scintillating vials, each containing 1 ml of solution and the corresponding sixth section of the series for a total of eight sections (make sure the sections are all submerged in the solution). This way, vial 1 will have sections 1, 7, 13, and so on; vial 2 will have sections 2, 8, 14, and so on.
3. Rinse the sections once or twice (to remove excess fluorescent particles).
4. Searching for the cell: Arrange the 48 sections individually in rostrocaudal order. (This can be done in two 24-well dishes.) Then mount the first section onto a glass slide and search for the cell under a epifluorescence microscope. Do not cover the section with a glass coverslip and do not use anything to enhance fluorescence. Just keep the section wet with cold PBS. These additional steps may substantially deteriorate the tissue and diminish the ability to do lengthy processing. If you do not find the cell, jump 150 μm and mount the fourth section and repeat the process. Instead of scanning sections in order, this speeds up the process of finding the cell; usually you will find dendritic processes and then you can just follow them very quickly (maybe through several sections) to the soma.
5. Document your finding by taking photographs, maybe at two or three different magnifications, usually 5×, 20×, and 40×. Low-magnification pictures can quickly determine the region where the cell is located.

More than 40× may be difficult because of the focusing over wet mounted tissue. Fluorescence may be very intense so that the soma may appear larger and blurry. Try to minimize this by illuminating at less than 100% and by using filters. At this time one can also determine if the cell is double labeled for instance with Fluorogold.

Note: We suggest using red fluorescent markers to label single cells because the normal human eye is more capable of detecting red than any other color.

G. Neurochemical Identification of Biocytin-Filled Neuron

Day 5

1. Incubate the section with the soma and a second control section selected from the ones in storage in a monoclonal rat anti-ChAT antibody (Rat anticholine acetyltranferase; 1:10; 2 days at 4°C; Boehringer Mannheim, Germany). Triton X can be added to help penetration of the antibodies and improve chances of positive immunotest, i.e., 0.02% Triton X in 0.1 M PB. This, however, may render the section useless for EM. Store the rest of the sections in 0.1 M PBS at 4°C or proceed to develop them (see conversion of fluorescent signal to DAB).
2. Rinse the section with the soma and the control section.
3. Incubate in a secondary antibody conjugated to, for instance, fluorescein isothiocyanate (FITC-conjugated goat anti-rat; 1:100–200; 4 h at room temperature; Jackson ImmunoResearch Labs, West Grove, PA). If the results of the incubation are poor, i.e., the fluorescent signal is not very good, the incubation can be done overnight at 4°C in a shaker. The problem is that in serial testing for different immunochemicals, this can add substantial time to the processing.

Day 6

Locate again the single-labeled cell with the "red" excitation/emission filter set of the fluorescence microscope and photograph it; change filters and determine if the same cell also emits green fluorescent light. If it does, then this is evidence that the juxtacellularly labeled cell expresses ChAT and it should be photographed again. If the identified cell is not ChAT positive, one can repeat the steps using a different primary antibody and a different control section. This procedure can be repeated two or three times. The secondary antibody can always be conjugated to FITC or some other "green" fluorochrome. This does not confound the results because one can observe how additional cells appear under "green" fluorescence in the field of interest, including or not the identified neuron. The latter neuron remains the only cell visible through the "red" fluorescence filter set.

H. Conversion of the Fluorescent Signal to DAB

1. Incubate the section containing the soma and all adjacent sections of interest (that were processed in avidin-conjugated rhodamine) in biotinylated peroxidase [1:200, "B" component of standard ABC (Avidin–Biotin Peroxidase complex) kit] (Vector Laboratories Inc., Burlingame, CA) for 2–4 h at room temperature (RT). The "A" or avidin component of the ABC kit is omitted because the single-stained neuron already contains the avidin (from the avidin-conjugated rhodamine).
2. Develop the neuron using 3,3′-diaminobenzidine tetrahydrochloride as a chromogen intensified with nickel (Ni) by incubating the sections for 10 min in a solution containing 0.05% DAB and 0.038% nickel ammonium sulfate and then adding hydrogen peroxide to a final concentration of 0.01%, while agitating for another 10–20 min. To determine the best timing, periodically wet mount the section with the soma or one with dendrites and see how dark they are using a regular transmitted light microscope. Try to balance the result between a very dark signal and a very low background. The overall darkness of the section containing the soma may be different because of the extra processing.
3. Rinse thoroughly to get rid of any Ni-DAB deposits outside the labeled neuron.

Note: The development of DAB can also be done by using 10% B-D-glucose and glucose oxidase instead of hydrogen peroxide. In short, after incubating the sections in the "B" component of the ABC kit as described above, incubate sections (15–25 min at RT) in a solution of 0.1 M PB containing 50 mg DAB, 40 mg ammonium chloride, 40 mg nickel ammonium sulfate, 0.4 mg glucose oxidase, and 200 mg B-D-glucose per 100 ml of solution. If one desires to filter the solution, this must be done before adding the glucose oxidase.

I. Staining for a Second Antigen

Days 7 and 8

1. *Select the section*: If the single cell was ChAT positive and one wants to double label the material, in order to find out if axon collaterals of the cholinergic neuron contact, for example, NPY neurons, then several sections around the soma of the cholinergic cell should be selected.
2. Incubate the sections in a primary antibody (Rabbit anti-NPY; 1:500; 2 days at 4°C; Peninsula Laboratories, Inc., Belmont, CA).
3. Rinse sections two or three times, then incubate in secondary antibody (Biotinylated Goat anti-Rabbit 1:200, 4 h RT; Jackson ImmunoResearch Labs, West Grove, PA).

4. Incubate in ABC as indicated in the ABC kit. Develop as described above, but using DAB only, without nickel enhancement. Develop long enough to make the signal light brown. Do not overdevelop because then it will be difficult to distinguish black from brown.

Note: If there are any concerns about again using avidin and biotin because of the possible detection of false signals beforehand, sections can be blocked using the avidin–biotin blocking agents sold by Vector (follow instructions in the package) or the signal can be developed by the peroxidase antiperoxidase (PAP) technique (see Pickel and Milner, 1989).

J. Embedding for Electron Microscopy

Days 9 and 10

1. Osmification: Sections to be investigated at the EM level should be osmicated in a solution containing 1% osmium tetroxide (Electron Microscopy Sciences, Fort Washington, PA) in phosphate-buffered saline (PBS), for approximately 30–40 min.
2. Dehydrate tissue in an ascending series of ethanols (30, 50, 70, 90, 100%). Do contrasting by treating the tissue with 1% uranyl acetate (Electron Microscopy Sciences, Fort Washington, PA) in 70% ethanol, for 30 min.
3. Dehydrate tissue with 1% propylene oxide (Electron Microscopy Sciences, Fort Washington, PA).
4. Infiltrate sections in durcupan (Fluka Chemie AG, Buchs, Switzerland) overnight and then flat embed them between liquid release agent-coated (Electron Microscopy Sciences, Fort Washington, PA) microscope glass slides and coverslips.

K. 3D Light Microscopy Reconstructions

Days 11–30

Neuron reconstructions at the light microscopy level can be carried out using several methods. Because 3D reconstruction offers more information than do 2D reconstructions obtained with typical camera lucida systems, it is advantageous to use a computerized 3D neuron tracing system such as the one offered by MicroBrightField Inc. (Williston, VT). Starting from the soma, the entire neuron is reconstructed from serial sections. The number of sections used in each case varies according to the cell. In the case of double-labeled material it is convenient to also plot other neurons, which are in close proximity to the axon of the juxtacellularly label cell. In the cases presented here the Neurolucida hardware system was interfaced with a Zeiss Axioscope

microscope. Outlines of the sections, contours of structures, and fiducial markers were drawn with a 5× Plan-NEOFLUAR objective lens. Somata, dendritic, and axonal branches were traced with a 100×, oil immersion ACHROPLAN objective lens.

L. Electron Microscopy and 3D Reconstruction from Ultrathin Sections

Days 31–40

After photography and full serial reconstruction of the labeled neuron, coverslips can be removed and pieces of interest are dissected out of the tissue with a razor blade. Small pieces of tissue containing areas of interest (such as boutons) are mounted onto blank durcupan blocks and trimmed appropriately. Ribbons of ultrathin sections are cut on a Reichert Ultracut E ultramicrotome and picked up onto Formvar-coated single-slot grids (Electron Microscopy Sciences, Fort Washington, PA). In our examples, the ultrathin sections were analyzed on a Tecnai 12 transmission electron microscope and pictures were captured using either a Gatan Ultrascan digital camera US 4000 SP (11,000×) or conventional EM film. The films were developed and then digitized using a Microtek Scanmaker 4 scanner and further manipulated using Photoshop.

a. Ultrathin cutting

1. Set the block into the holder and using a blade trim it roughly.
2. Under the light microscope, determine the depth in which the area of interest is. With a glass knife, cut away the layers superficial to the area of interest.
3. Using a glass knife, trim the block.
4. Begin to cut ultrathin sections using a diamond knife with simultaneous light microscopic control.
5. Mount sections onto Formvar-coated single-slot grids (copper for general purposes or nickel if intending to do postembedding procedures).
6. Dry grids with filter paper and then place them into gridboxes.

Days 41–60

For quantifying synaptic contacts on electrophysiologically identified neurons, a certain portion of the dendritic tree or of the chemically and electrophysiologically identified neuron has to be reconstructed and the total number of synapses can be extrapolated knowing the total dendritic length and the number of synaptic boutons in the reconstructed volume. The small

dendritic segment of the parvalbumin neuron shown in Fig. 7.12 was reconstructed from 66 ultrathin sections. The collection of digital images took about 20 EM h and about 10-h computer time was needed to reconstruct it in 3D.

Acknowledgments. The research summarized in this review was supported by NIH grant NSO23945 to LZ and IR25 GM60826 to LZ and AD. The Tecnai 12 electron microscope was purchased from grant S10 RR13959 (LZ). Special thanks are due to Lennart Heimer for his comments on a previous version of this manuscript.

REFERENCES

Aghajanian, G. K., and Vandermaelen, C. P., 1982, Intracellular identification of central noradrenergic and serotonergic neurons by a new double labeling procedure, *J. Neurosci.* **2:**1786–1792.

Alonso, A., Khateb, A., Fort, P., Jones, B. E., and Muhlethaler, M., 1996, Differential oscillatory properties of cholinergic and noncholinergic nucleus basalis neurons in guinea pig brain slice, *Eur. J. Neurosci.* **8:**169–182.

Arbib, M. A., Erdi, P., and Szentágothai, J., 1998, *Neural Organization: Structure, Function, and Dynamics*, Cambridge: The MIT Press, p. 407.

Blackstad, T. W., 1965, Mapping of experimental axon degeneration by electron microscopy of Golgi preparations, *Z. Zellforsch. Mikrosk. Anat.* **67:**819–834.

Buhl, E. H., 1993, Intracellular injection in fixed slices in combination with neuroanatomical tracing techniques and electron microscopy to determine multisynaptic pathways in the brain, *Microsc. Res. Tech.* **24:**15–30.

Cajal, S. R., 1911, *Histologie du Système nerveux de l'Homme et des Vertébrés*, Paris: A Maloine.

Cullheim, S., and Kellerth, J. O., 1978, A morphological study of the axons and recurrent axon collaterals of cat sciatic alpha-motoneurons after intracellular staining with horseradish peroxidase, *J. Comp. Neurol.* **178:**537–557.

Detari, L., 2000, Tonic and phasic influence of basal forebrain unit activity on the cortical EEG, *Behav. Brain Res.* **115:**159–170.

Detari, L., and Vanderwolf, C. H., 1987, Activity of identified cortically projecting and other basal forebrain neurones during large slow waves and cortical activation in anaesthetized rats, *Brain Res.* **437:**1–8.

Dringenberg, H. C., and Vanderwolf, C. H., 1998, Involvement of direct and indirect pathways in electrocorticographic activation, *Neurosci. Biobehav. Rev.* **22:**243–257.

Duque, A., Balatoni, B., Detari, L., and Zaborszky, L., 2000, EEG correlation of the discharge properties of identified neurons in the basal forebrain, *J. Neurophysiol.* **84:**1627–1635.

Fairen, A., Peters, A., and Saldanha, J., 1977, A new procedure for examining Golgi impregnated neurons by light and electron microscopy, *J. Neurocytol.* **6:**311–337.

Freund, T. M., and Somogyi, P., 1989, Synaptic relationships of Golgi-impregnated neurons as identified by electrophysiological or immunocytochemical techniques, In: Heimer, L., and Zaborszky, L. (eds.), *Neuroanatomical Tract-Tracing Methods 2*, New York: Plenum Press, pp. 201–238.

Glaser, J. R., and Glaser, E. M., 1990, Neuron imaging with Neurolucida—a PC-based system for image combining microscopy, *Comput. Med. Imaging Graph.* **14:**307–317.

Golgi, C., 1883, Recherches sur l'histologie des centers nerveux, *Arch. Ital. Biol.* **3:**285–317.

Grace, A. A., and Bunney, B. S., 1983a, Intracellular and extracellular electrophysiology of nigral dopaminergic neurons—1. Identification and characterization, *Neuroscience* **10:** 301–315.

Grace, A. A., and Bunney, B. S., 1983b, Intracellular and extracellular electrophysiology of nigral dopaminergic neurons—2. Action potential generating mechanisms and morphological correlates, *Neuroscience* **10:**317–331.

Graham, R. C., Jr., and Karnovsky, M. J., 1966, The early stages of absorption of injected horseradish peroxidase in the proximal tubules of mouse kidney: ultrastructural cytochemistry by a new technique, *J. Histochem. Cytochem.* **14:**291–302.

Jankowska, E., Rastad, J., and Westman, J., 1976, Intracellular application of horseradish peroxidase and its light and electron microscopical appearance in spinocervical tract cells, *Brain Res.* **105:**557–562.

Kita, H., and Armstrong, W., 1991, A biotin-containing compound *N*-(2-aminoethyl)biotinamide for intracellular labeling and neuronal tracing studies: comparison with biocytin, *J. Neurosci. Methods* **37:**141–150.

Kitai, S. T., Kocsis, J. D., Preston, R. J., and Sugimori, M., 1976a, Monosynaptic inputs to caudate neurons identified by intracellular injection of horseradish peroxidase, *Brain Res.* **109:**601–606.

Kitai, S. T., Kocsis, J. D., and Wood, J., 1976b, Origin and characteristics of the cortico-caudate afferents: an anatomical and electrophysiological study, *Brain Res.* **118:**137–141.

Koos, T., and Tepper, J. M., 1999, Inhibitory control of neostriatal projection neurons by GABAergic interneurons, *Nat. Neurosci.* **2:**467–472.

Koos, T., and Tepper, J. M., 2002, Dual cholinergic control of fast-spiking interneurons in the neostriatum, *J. Neurosci.* **22:**529–535.

Kristensson, K., and Olsson, Y., 1971, Retrograde axonal transport of protein, *Brain Res.* **29:**363–365.

LaVail, J. H., and LaVail, M. M., 1972, Retrograde axonal transport in the central nervous system, *Science* **176:**1416–1417.

Li, Y., Brewer, D., Burke, R. E., and Ascoli, G. A., 2005, Developmental changes in spinal motoneuron dendrites in neonatal mice, *J. Comp. Neurol.* **483**(3):304–317.

Light, A. R., and Durkovic, R. G., 1976, Horseradish peroxidase: an improvement in intracellular staining of single, electrophysiologically characterized neurons, *Exp. Neurol.* **53:**847–853.

Lynch, G., Deadwyler, S., and Gall, C., 1974a, Labeling of central nervous system neurons with extracellular recording microelectrodes, *Brain Res.* **66:**337–341.

Lynch, G., Gall, C., Mensah, P., and Cotman, C. W., 1974b, Horseradish peroxidase histochemistry: a new method for tracing efferent projections in the central nervous system, *Brain Res.* **65:**373–380.

McMullen, N. T., and Glaser, E. M., 1988, Auditory cortical responses to neonatal deafening: pyramidal neuron spine loss without changes in growth or orientation, *Exp. Brain Res.* **72:**195–200.

Nambu, A., and Llinas, R., 1997, Morphology of globus pallidus neurons: its correlation with electrophysiology in guinea pig brain slices, *J. Comp. Neurol.* **377:**85–94.

Nunez, A., 1996, Unit activity of rat basal forebrain neurons: relationship to cortical activity, *Neuroscience* **72:**757–766.

Pang, K., Tepper, J. M., and Zaborszky, L., 1998, Morphological and electrophysiological characteristics of noncholinergic basal forebrain neurons, *J. Comp. Neurol.* **394:**186–204.

Pickel, V., and Milner, T. A., 1989, Interchangeable uses of autoradiographic and peroxidase markers for electronmicroscopic detection of neuronal pathways and transmitter-related antigens in single sections, In: Heimer, L., and Zaborszky, L. (eds.), *Neuroanatomical Tract-Tracing Methods 2*, New York: Plenum Press, pp. 97–128.

Pinault, D., 1994, Golgi-like labeling of a single neuron recorded extracellularly, *Neurosci. Lett.* **170:**255–260.

Pinault, D., 1996, A novel single-cell staining procedure performed in vivo under electrophysiological control: morpho-functional features of juxtacellularly labeled thalamic cells and other central neurons with biocytin or Neurobiotin, *J. Neurosci. Methods* **65:** 113–136.

Reiner, A., Veenman, C. L., Medina, L., Jiao, Y., Del Mar, N., and Honig, M. G., 2000, Pathway tracing using biotinylated dextran amines, *J. Neurosci. Methods* **103:**23–37.

Renuka, and Dani, H. M., 1983, Effects of toxic doses of urethane on rat liver and lung microsomes, *Toxicol. Lett.* **15:**61–64.

Richards, C. D., 1972, On the mechanism of barbiturate anaesthesia, *J. Physiol.* **227:**749–767.

Rogers, R. C., Butcher, L. L., and Novin, D., 1980, Effects of urethane and pentobarbital anesthesia on the demonstration of retrograde and anterograde transport of horseradish peroxidase, *Brain Res.* **187:**197–200.

Schmued, L. C., 1994, Anterograde and retrograde neuroanatomical tract tracing with fluorescent compounds, *Neurosci. Protoc.* **50:**1–15.

Schmued, L. C., and Heimer, L., 1990, Iontophoretic injection of fluoro-gold and other fluorescent tracers, *J. Histochem. Cytochem.* **38:**721–723.

Schmued, L., Kyriakidis, K., and Heimer, L., 1990, In vivo anterograde and retrograde axonal transport of the fluorescent rhodamine-dextran-amine, Fluoro-Ruby, within the CNS, *Brain Res.* **526:**127–134.

Scorcioni, R., Lazarewicz, M. T., and Ascoli, G. A., 2004, Quantitative morphometry of hippocampal pyramidal cells: differences between anatomical classes and reconstructing laboratories, *J. Comp. Neurol.* **473**(2):177–193.

Simon, L., Noszek, A., Garab, S., and Zaborszky, L., 2005, Optimal alignment of EM serial sections. Program No. 458.113.2005. *Abstract Viewer/Itinerary Planner.* Washington, DC: Society for Neuroscience. Online.

Snow, P. J., Rose, P. K., and Brown, A. G., 1976, Tracing axons and axon collaterals of spinal neurons using intracellular injection of horseradish peroxidase, *Science* **191:**312–313.

Somogyi, P., 1977, A specific "axo-axonal" interneuron in the visual cortex of the rat, *Brain Res.* **136:**345–350.

Somogyi, P., and Freund, T. M., 1989, Immunocytochemistry and synaptic relationships of physiologically characterized HRP-filled neurons, In: Heimer, L., and Zaborszky, L. (eds.), *Neuroanatomical Tract-Tracing Methods 2*, New York: Plenum Press, pp. 239–264.

Stepanyants, A., Tamas, G., and Chklovskii, D. B., 2004, Class-specific features of neuronal wiring, *Neuron* **43**(2):251–259.

Szentágothai, J., 1970, Glomerular synapses, complex synaptic arrangements, and their operational significance, In: Schmitt, F. O. (ed.), *The Neurosciences: Second Study Program*, New York, NY: The Rockefeller University Press, pp. 427–443.

Szentágothai, J., 1978, The neuron network of the cerebral cortex: a functional interpretation, *Proc. R. Soc. Lond. B* **201:**219–248.

Yuasa, H., and Watanabe, J., 1994, Influence of urethane anesthesia and abdominal surgery on gastrointestinal motility in rats, *Biol. Pharm. Bull.* **17:**1309–1312.

Zaborszky, L., Csordas, A., Buhl, D., Duque, A., Somogyi, J., and Nadasdy, Z., 2002, Computational anatomical analysis of the basal forebrain corticopetal system, In: Ascoli, A. (ed.), *Computational Neuroanatomy: Principles and Methods*, NJ: Humana Press, pp. 171–197.

Zaborszky, L., and Duque, A., 2000, Local synaptic connections of basal forebrain neurons, *Behav. Brain Res.* **115:**143–158.

Zaborszky, L., Leranth, C., Makara, G. B., and Palkovits, M., 1975, Quantitative studies on the supraoptic nucleus in the rat: II. Afferent fiber connections, *Exp. Brain Res.* **22:**525–540.

Zaborszky, L., Palkovits, M., and Flerko, B., 1992, Janos Szentágothai: a life-time adventure with the brain. An appreciation on his eightieth birthday, *J. Comp. Neurol.* **326:**1–6.